NUREG/CR-1057
PNL-3219
RH

Confirmation of Conversion Factors Relating Exposure and Dose-Equivalent Index Presented in ANSI N13.11

R. C. Yoder
W. T. Bartlett
J. W. Courtney
C. D. Hooker
J. A. Holland
B. T. Hogan

November 1979

Prepared for
the U.S. Nuclear Regulatory Commission

Pacific Northwest Laboratory
Operated for the U.S. Department of Energy
by Battelle Memorial Institute

PNL-3219

Battelle

PACIFIC NORTHWEST LABORATORY
operated by
BATTELLE
for the
UNITED STATES DEPARTMENT OF ENERGY
Under Contract EY-76-C-06-1830

Printed in the United States of America
Available from
National Technical Information Service
United States Department of Commerce
5285 Port Royal Road
Springfield, Virginia 22151
Price: Printed Copy $____*; Microfiche $3.00

*Pages	NTIS Selling Price
001-025	$4.00
026-050	$4.50
051-075	$5.25
076-100	$6.00
101-125	$6.50
126-150	$7.25
151-175	$8.00
176-200	$9.00
201-225	$9.25
226-250	$9.50
251-275	$10.75
276-300	$11.00

NUREG/CR-1057
PNL-3219
RH

CONFIRMATION OF CONVERSION FACTORS RELATING EXPOSURE AND DOSE-EQUIVALENT INDEX PRESENTED IN ANSI N13.11

R. C. Yoder
W. T. Bartlett[a]
J. W. Courtney
C. D. Hooker
J. A. Holland
B. T. Hogan

November 1979

Prepared for
the U.S. Nuclear Regulatory Commission
under a Related Services Agreement
with the U.S. Department of Energy
Contract EY-76-C-06-1830
FIN No. 300 AO 1255

Pacific Northwest Laboratory
Richland, Washington 99352

(a) Chappel Hill, Texas

ACKNOWLEDGMENTS

The authors wish to acknowledge Robert Alexander of the U.S. Nuclear Regulatory Commission, Office of Standards Development, as the program sponsor of this research. Appreciation is extended to N. R. Gordon and W. E. Skiens of Pacific Northwest Laboratory's Materials Department for their assistance in the development of the tissue-equivalent plastic and the extrapolation chamber. The authors also wish to acknowledge and extend special appreciation to J. L. Baer for her excellent editorial assistance in the preparation of this report.

ABSTRACT

Conversion factors relating dose-equivalent index (DEI) and exposure were derived from experimental measurements. Conversion factors for computing both the deep and shallow dose-equivalent indices are presented. These conversion factors were derived for K-fluorescence x-rays with energies less than 100 keV and for National Bureau of Standards (NBS) filtered x-rays with effective energies less than 200 keV. The dose-equivalent measurements were made using a tissue-equivalent phantom with an incorporated extrapolation chamber. The experimentally derived DEI conversion factors were compared with DEI conversion factors presented in draft standard N13.11, July 1978, of the American National Standards Institute (ANSI). Notable differences were found between the conversion factors in ANSI N13.11 and those derived for K-fluorescence x-rays. The conversion factors for NBS filtered x-rays compared somewhat better with the ANSI conversion factors.

SUMMARY

Conversion factors that relate exposure and dose-equivalent index (DEI) have been presented in Draft American National Standard for Testing Personnel Dosimetry Performance, ANSI N13.11 (American National Standards Institute 1978). These conversion factors can provide comparability in the assignment of DEI values to irradiated personnel dosimeters. When the draft standard is approved, the DEI conversion factors will be used to evaluate the performance of dosimeter processors and will influence the magnitude of assigned occupational dose-equivalents. The accuracy of the conversion factors is therefore important.

The Pacific Northwest Laboratory contracted with the U.S. Nuclear Regulatory Commission (NRC) to confirm the DEI conversion factors presented in ANSI N13.11. The scope of the study was limited to confirming the conversion factors for photons with energies less than 200 keV. Both K-fluorescence x-ray and National Bureau of Standards (NBS) filtered x-ray techniques were used to produce photons.

Two types of conversion factors are presented in ANSI N13.11, Table 2. One type is for computing the shallow DEI or the dose-equivalent at 0.007-cm depth in a tissue-equivalent phantom. The other type is for computing the deep DEI or the dose-equivalent at 1-cm depth. Both types of conversion factors were examined in this study.

The experimental method used to derive DEI conversion factors consisted of making in-air exposure measurements and in-phantom dose-equivalent measurements. The in-air exposure measurements were made using a free-air ion chamber. The in-phantom measurements were made using an extrapolation chamber in a tissue-equivalent phantom.

The conversion factors derived from our experimental measurements differed from the conversion factors presented in ANSI N13.11 for both shallow and deep DEIs, and for both K-fluorescence and National Bureau of Standards filtered x-ray techniques. The differences were most noticeable when the ANSI conversion factors (which are given for monoenergetic photons) were compared with

the derived conversion factors for K-fluorescence x-rays. The pattern of differences between the K-fluorescence and the ANSI conversion factors was similar for the shallow dose-equivalent and the deep dose-equivalent; for all energies, the K x-ray conversion factors were higher than the ANSI conversion factors. The largest differences were apparent at the lower (16-keV) and higher (78- and 100-keV) photon energies, and for the deep dose-equivalent indices.

CONTENTS

ACKNOWLEDGMENTS iii

ABSTRACT v

SUMMARY vii

INTRODUCTION 1

CONCLUSIONS AND RECOMMENDATIONS 3

CONCEPT OF A CONVERSION FACTOR RELATING EXPOSURE AND DOSE-EQUIVALENT INDEX 5

CONVERSION FACTOR BASED ON ICRU DEFINITION OF DEI 5

EFFECTS OF GEOMETRY ON THE CONVERSION FACTOR 6

ALTERNATIVE APPROACHES TO A CONVERSION FACTOR. 8

APPROACHES TO IN-PHANTOM DOSIMETRY USING CAVITY IONIZATION THEORY . 11

CALIBRATED IONIZATION CHAMBERS 11

THERMOLUMINESCENT CAVITY CHAMBERS 12

EXTRAPOLATION CHAMBERS 12

DESIGN OF A TISSUE-EQUIVALENT PHANTOM WITH AN EXTRAPOLATION CHAMBER . 15

DEVELOPMENT OF A TISSUE-EQUIVALENT MATERIAL 16

THE EXTRAPOLATION CHAMBER 18

IRRADIATION METHODS 20

EXPERIMENTAL DESIGN 20

X-Ray Equipment 20

Determination of Beam Quality 22

MEASUREMENT TECHNIQUES AND NBS INTERCOMPARISONS 24

DETERMINATION OF DEI CONVERSION FACTORS 25

IN-AIR EXPOSURE CALIBRATIONS 25

MEASUREMENT OF DOSE-EQUIVALENT 25

CALCULATION OF CONVERSION FACTORS 27

DISCUSSION OF RESULTS 29

REFERENCES 34

APPENDIX A - HALF-VALUE LAYER AND SPECTROSCOPIC DATA A.1

APPENDIX B - TRANSMISSION OF K X-RAYS THROUGH TISSUE-EQUIVALENT PLASTIC B.1

APPENDIX C - CALIBRATION DATA C.1

APPENDIX D - CONVERSION FACTOR DATA D.1

APPENDIX E - TABULATED STOPPING-POWER DATA E.1

FIGURES

1	Extrapolation Chamber in a Tissue-Equivalent Phantom . . .	15
2	X-Ray Tube Head and Beam Control Devices	21
3	Typical Beam Uniformity Map	23
4	Comparison of K X-Ray and Filtered X-Ray Conversion Factors - Shallow DEI	30
5	Comparison of K X-Ray and Filtered X-Ray Conversion Factors - Deep DEI	30
6	Comparison of K X-Ray and ANSI Conversion Factors - Shallow DEI .	31
7	Comparison of K X-Ray and ANSI Conversion Factors - Deep DEI .	31
8	Comparison of Filtered X-Ray and ANSI Conversion Factors - Shallow DEI	32
9	Comparison of Filtered X-Ray and ANSI Conversion Factors - Deep DEI	32
A.1	Spectrum from NBS Technique LG	A.3
A.2	Spectrum from NBS Technique LI	A.3
A.3	Spectrum from NBS Technique LK	A.4
A.4	Spectrum from NBS Technique MFC	A.4
A.5	Spectrum from NBS Technique MFG	A.5
A.6	Spectrum from NBS Technique MFI	A.5
A.7	Spectrum from NBS Technique MFK	A.6
A.8	Spectrum from NBS Technique HFE	A.6
A.9	Spectrum from NBS Technique HFG	A.7
A.10	Spectrum from NBS Technique HFI	A.7
A.11	Spectrum from 16.1-keV K X-Ray	A.9
A.12	Spectrum from 23.7-keV K X-Ray	A.9
A.13	Spectrum from 34.3-keV K X-Ray	A.10

A.14 Spectrum from 43-keV K X-Ray A.10

A.15 Spectrum from 78-keV K X-Ray A.11

A.16 Spectrum from 100-keV K X-Ray A.11

A.17 Spectrum from Americium-241 . . . . . A.12

A.18 Spectrum from Americium-241 . . . . . A.12

B.1 Transmission Measurements for 23.7-keV K X-Rays B.2

B.2 Transmission Measurements for 34.3-keV K X-Rays B.2

B.3 Transmission Measurements for 43-keV K X-Rays B.3

B.4 Transmission Measurements for 58-keV K X-Rays B.3

B.5 Transmission Measurements for 78-keV K X-Rays B.4

TABLES

A.1 Comparison of NBS and PNL Filtered X-Ray Techniques . . . A.2

A.2 PNL K X-Ray Techniques A.8

D.1 Shallow DEI Data D.2

D.2 Deep DEI Data D.3

D.3 Derived DEI Conversion Factors for K X-Ray Techniques . . . D.4

D.4 Derived DEI Conversion Factors for NBS Filtered X-Ray Techniques . D.4

D.5 DEI Conversion Factors Presented in ANSI N13.11 . . . . D.5

CONFIRMATION OF CONVERSION FACTORS RELATING EXPOSURE AND DOSE-EQUIVALENT INDEX PRESENTED IN ANSI N13.11

INTRODUCTION

The Draft American National Standard Criteria for Testing Personnel Dosimetry Performance, ANSI N13.11 (American National Standards Institute 1978), presents a table of conversion factors for computing the dose-equivalent index (DEI) from exposure. The standard suggests two approaches to calibrating a photon beam in terms of exposure, an in-air calibration and an in-phantom calibration. A set of conversion factors for computing DEI was prepared by the ANSI standards committee for each calibration method. Each method, when used with the correct DEI conversion factor, should provide the same DEI.

Studies at the Pacific Northwest Laboratory (Bartlett et al. 1978) indicated that the two calibration approaches to determining DEI were not equivalent. Dose-equivalent indices calculated from in-air exposure measurements substantially differed from DEIs calculated from in-phantom measurements. The discrepancy was very apparent for photons with energies less than 200 keV and was not unexpected. The medical physics community has discussed a similar difference found with cobalt-60 calibrations (Friem and Feldman 1978).

Inaccuracies in the ANSI conversion factors may account for the differences found in the DEIs. The accuracy of DEI conversion factors is important because these conversion factors will be an integral part of assigning DEI values to irradiated personnel dosimeters. The ANSI N13.11 draft standard provides procedures for testing performance in routine personnel dosimetry under controlled conditions. Once the draft standard is approved, the prescribed methods for testing dosimetry performance will be used by a testing laboratory to evaluate the performance of dosimeter processors who provide a service in the determination of occupational radiation doses. A by-product of performance testing will be a more uniform approach to routine personnel dosimetry and, in particular, to dosimeter calibrations. Therefore, the conversion factors suggested in ANSI N13.11 will greatly influence the magnitude of permissible occupational radiation doses.

Because little published data is available from which to derive these conversion factors, experiments were needed to confirm the ANSI factors' adequacy. Pacific Northwest Laboratory (PNL)[a] therefore contracted with the U.S. Nuclear Regulatory Commission (NRC) to confirm the ANSI N13.11 conversion factors for photons with energies less than 200 keV. The scope of the study was limited to the conversion factors relating in-air exposure and DEI. Accurate in-phantom measurements of exposure to low-energy photons, made using calibrated ionization chambers, are extremely difficult to obtain at the very shallow depths where the maximum dose-equivalent usually occurs. Correction factors accounting for perturbation of the photon and electron fields by the chamber in the phantom have not been thoroughly investigated. Consequently, we concentrated our efforts on in-air conversion factors.

Empirical determinations of DEI conversion factors for low-energy photons are complex and difficult to attain accurately. Subtle variations in the application of the DEI concept and in the measurement of the DEI may significantly influence the value of the conversion factors. Particularly important are geometrical or spatial considerations, the selection of tissue-equivalent materials, and the measurement techniques used to determine absorbed dose in the tissue-equivalent material.

The impact of these variables is discussed in the first two sections of this report to emphasize the complexity of the DEI measurements and to define the irradiation conditions for which our conversion factors apply. We assume that the reader has a basic knowledge of the quantities and concepts used in personnel dosimetry and personnel dosimetry calibrations. We do not attempt to justify the use of the DEI concept (which is discussed by the International Commission on Radiation Units and Measurements (ICRU) [1976]); rather, we describe the precautions that must be taken if DEI conversion factors are to be used in radiation protection. The equipment and conditions we used to determine DEI conversion factors follow this discussion, along with the results of the study.

(a) Operated for the U.S. Department of Energy by Battelle Memorial Institute.

CONCLUSION AND RECOMMENDATIONS

The calibration of personnel dosimeters in terms of dose-equivalent index introduces several considerations. Because the DEI for low-energy photons occurs near the surface of a tissue-equivalent material, in-phantom measurements of exposure require special instruments and techniques. Consequently, in-air measurements of exposure are preferred for routine calibrations and dosimeter testing. The accuracy of the calibrations and testing will be influenced by errors in the conversion factors that relate exposure and dose-equivalent index. These factors are therefore of primary importance.

Little information about the derivation of low-energy photon conversion factors is available in the literature. Many assumptions and complex calculations were used by the ANSI N13.11 standards committee in establishing their DEI conversion factors. Therefore, differences between their conversion factors and our experimental data were not unexpected. The main conclusions and recommendations resulting from this study are presented below.

- The ANSI N13.11 DEI conversion factors can be compared with experimentally derived conversion factors. Such a comparison with our experimental factors indicated the ANSI factors to be most suitable for filtered x-ray spectra. New conversion factors for monoenergetic photons should be developed for the final draft of the ANSI N13.11 standard.
- The incorporation of an extrapolation chamber into a tissue-equivalent phantom is a satisfactory alternative to calibrated ionization chambers for measuring in-phantom absorbed dose.
- Additional experimental information on the exact depth of the maximum dose-equivalent is needed. We studied only the two depths, 0.007 cm and 1 cm, defined in ANSI N13.11 paragraph 2.4. Depth dose information for K-fluorescence and National Bureau of Standards (NBS) filtered x-rays would be useful in the design of personnel dosimeters.
- Field size can influence the amount of photon scatter. Very wide beams represent real field conditions. However, such beams can cause

problems in the laboratory; beam uniformity is of special concern. Therefore, specifications for beam uniformity are needed to assure more comparability in personnel dosimeter testing. In addition, the effect of field size for low-energy photons should be investigated to determine the beam size that provides the best balance between the need to simulate real field conditions (wide beams) and the need for beam uniformity (narrow beams).

- K-fluorescence x-rays, which are nearly monenergetic, should be used in dosimeter calibrations, in addition to the NBS filtered techniques. Much of the information on interaction and absorption coefficients is described for monoenergetic photons. The averaging needed to evaluate the effective attenuation and absorption coefficients of the filtered spectra adds complexity to dosimetry calculations.
- The influence of the phantom's shape on DEI conversion factors should be investigated because the shape affects scatter. The DEI is defined for a spherical phantom; however, a square phantom is more practical for exposing dosimeters. The difference between scatter in a spherical phantom and scatter in a square phantom is not known.
- For moderate- and high-energy photons, in-phantom calibrations in terms of absorbed dose are preferable to in-air exposure calibrations. In-air calibrations should be used for low-energy photons.
- Careful review of all new information on DEI conversion factors is warranted so that a universal set of conversion factors can be obtained for dosimeter testing.

CONCEPT OF A CONVERSION FACTOR RELATING EXPOSURE AND DOSE-EQUIVALENT INDEX

The basic purpose of an exposure-to-DEI conversion factor is to relate a value measured in air (i.e., exposure) to a value measured in a tissue simulant (i.e., the maximum rem, or DEI). Exposure can be measured relatively easily and very accurately, with excellent precision or repeatability. Measurement of the DEI is much more difficult, but the use of a conversion factor eliminates the need for this measurement. Once the conversion factor is known, one can measure an exposure from a beam of photons and calculate, using the conversion factor, the DEI that occurs when a 30-cm-dia sphere of tissue-equivalent material is placed in the same beam of photons.

Exposure measurements have been used by calibration laboratories to provide routine photon beam calibrations that are traceable to a primary standard. The use of exposure provides a common reference point, enabling comparisons among calibration laboratories. However, the DEI concept is more closely related to the information needed in radiation protection than is exposure. The use of conversion factors allows the calibration of personnel dosimeters in terms of their ability to measure DEI, while maintaining the accuracy achieved by exposure measurements. The need for comparabililty was an underlying reason for the development of ANSI N13.11. Since conditions and analysis methods vary from one calibration laboratory to the next, it is essential that universally applicable conversion factors be developed if dosimetry performance is to be compared across the laboratories.

CONVERSION FACTOR BASED ON ICRU DEFINITION OF DEI

Consider a particular reference point located in a mass of air irradiated by low-energy photons. With appropriate instruments, the exposure at this point can be determined. The DEI for the reference point is defined as the maximum dose-equivalent within a 30-cm-dia sphere of tissue-equivalent material centered at the reference point (ICRU 1971). The value of the DEI conversion

factor for the reference point is the DEI, or the maximum dose-equivalent found in the sphere, divided by the exposure at the reference point. The conversion factor is typically expressed in terms of rem/R.

An important consideration arises when the DEI is used (ICRU 1976): the location of the reference point at which exposure was measured and for which the DEI value is defined is different from the location at which the maximum dose-equivalent occurs. Generally, the location of the maximum dose-equivalent is 14 to 15 cm away from the reference point in the direction of the photon source. Therefore, a geometrical concern is introduced, as explained below.

EFFECTS OF GEOMETRY ON THE CONVERSION FACTOR

From an exposure measurement made in air, the maximum dose-equivalent in a tissue-equivalent phantom can be calculated using a basic dosimetric equation:

$$rem_{max} = X \cdot BSF \cdot f \cdot QF \qquad \text{(Eq. 1)}$$

where:

X is the exposure in air at the location of the maximum dose-equivalent,

BSF is the backscatter factor,

f is a factor to convert R to absorbed dose in tissue, expressed as rads, and

QF is a quality factor to convert rads in tissue to dose-equivalent, expressed as rem.(a)

The backscatter factor corrects for the dose due to scatter from surrounding material and is specific for the depth in the phantom at which maximum electronic equilibrium occurs. This depth is usually referred to as d_{max}.

(a) A detailed discussion of all the terms in the equation goes beyond the scope of this report; however, excellent discussions are available in the literature (Johns and Cunningham 1974; ICRU 1976).

For photon energies above 200 keV, d_{max} is the depth or location of the maximum dose-equivalent. Photons with energies less than 200 keV produce a maximum dose-equivalent at a depth different from d_{max}, but the difference between the dose-equivalents at the two depths is so slight (Johns and Cunningham 1974) as to be negligible for the purposes of this discussion.

Returning to the determination of a conversion factor in a 30-cm-dia sphere of tissue-equivalent material, if exposure is measured in air at the reference point, P_R, the DEI conversion factor can be given from Equation 1 as:

$$\frac{rem}{R} = \frac{X_1 \cdot BSF \cdot f \cdot QF}{X_R} \qquad \text{(Eq. 2)}$$

where:

X_1 is the exposure measured in air at the point where d_{max} in the phantom occurs, and

X_R is the exposure measured in air at the reference point, P_R.

This equation shows the dependence of the DEI conversion factor on the ratio of the exposure at d_{max} in the phantom to the exposure at the reference point. Any change in this ratio will change the DEI conversion factor.

The ratio of the exposures found at D_{max} and P_R depends on the distance between the two points. When a 30-cm-dia sphere of tissue-equivalent material is used, the points are 14 to 15 cm apart.[(a)] Unfortunately, the variation in exposure between points in space is not constant in any one calibration laboratory, but changes with the distance to the photon source (because of the inverse square law) and with the methods used to generate photons. In fact, the variation in exposure as a function of the distance to the photon source

(a) The distance between D_{max} and P_R does not change appreciably with changing photon energy for the low energies used in this study.

may be unique in each laboratory because of the x-ray techniques used by the laboratory. A DEI conversion factor that reflects geometrical considerations may, therefore, not be universally applicable.

ALTERNATIVE APPROACHES TO A CONVERSION FACTOR

Two approaches can be used to produce DEI conversion factors that are not dependent on a specific irradiation geometry. One approach is to create a broad parallel beam of photons. Such a beam does not exhibit inverse square variations between points. The advantage of using this type of beam is that the exposure ratio for any points separated by distances applicable to the DEI concept (30 cm) is unity, assuming that air attenuation and buildup are negligible. Because $X_1 = X_R$, the DEI conversion factor presented earlier (Equation 2) becomes:

$$\frac{rem}{R} = BSF \cdot f \cdot QF \qquad \text{(Eq. 3)}$$

Notice that an exposure measurement at the reference point is not required for use of this conversion factor; any point in the broad parallel photon beam can be used for the exposure measurement.

A review of Appendix C of ANSI N13.11 indicates that the DEI conversion factors presented in Table 2 of the standard were developed for a broad parallel photon beam and do not reflect any spatial changes in the beam. However, the source-to-phantom distances and source sizes commonly used in laboratories do not result in a broad parallel beam at the phantom, primarily because of the inverse square relation between exposure and distance to the source. When low-energy photons are used, air attenuation may also be significant, thus adding to the variation in exposure between points. For these reasons, ANSI's DEI conversion factors should not be used to relate exposures at two separate points, P_R and D_{max}.

The second approach to developing a conversion factor that minimizes geometry relates the maximum dose-equivalent to exposure when both are evaluated

at the same point in space. The reference point is considered to be at the location of d_{max}, rather than at the center of the tissue-equivalent sphere. The DEI conversion factor (Equation 2) is then reduced to:

$$\frac{rem}{R} = BSF \cdot f \cdot QF \qquad \text{(Eq. 4)}$$

because X_1 and X_R are measured in air at the same point and are therefore identical. Note that this equation is the same as the one developed for the broad parallel beam (Equation 3): DEI conversion factors developed from the two alternative approaches are comparable. Because in this second approach the exposure is measured at the point of the maximum dose-equivalent, the influence of the spatial variation of exposure is largely eliminated. For most source-to-phantom distances used in the laboratory, a conversion factor developed in this manner is more applicable than the parallel beam conversion factor. However, a conversion factor based on a broad parallel beam, such as that developed by ANSI, could be used even in a laboratory where the photon beam was not parallel as long as the exposure calibration was performed at the location of the maximum dose-equivalent instead of at the center of the tissue-equivalent sphere.

The approach of measuring dose-equivalent and exposure at the same point is not new. This type of DEI conversion factor was suggested for use in evaluating environmental monitors in paragraph 44 of Conceptual Basis for the Determination of Dose Equivalent (ICRU 1976). In addition, DEI conversion factors based on this definition would be analogous to the tissue-air ratio (TAR) used in radiation therapy calculations (Johns and Cunningham 1974). In fact, the backscatter factor is the TAR at a depth of d_{max}. Given this background of use and the broad applicability of a conversion factor derived in this way, we define "DEI conversion factor" as used in the rest of this report to mean the ratio of the maximum dose-equivalent (rem) to the exposure measured in air when both quantities are evaluated at the same location in space.

Experimentally measuring the maximum dose-equivalent in a phantom requires prior knowledge of the depth at which this maximum will occur. The depth will vary as a function of photon energy and the energy spectrum. To account for

this depth variation, ICRU (1976) extended the concept of the dose-equivalent index, dividing the tissue-equivalent sphere into two shells and a core. The outer shell extends from the surface of the sphere to a depth of 0.007 cm. The inner shell extends from 0.007 cm to a depth of 1 cm. The remainder of the sphere is considered the core. The maximum dose-equivalents in the core and the adjacent surrounding shell are called the deep and shallow dose-equivalent indices, or the restricted dose-equivalent indices (ICRU 1976). Paragraph 2.4 of ANSI N13.11 defines the shallow and deep DEIs as "equal to the dose equivalents in the human body or phantom at depths of 0.007 cm and 1.0 cm, respectively." Based on this definition, we designed our study to measure the dose-equivalents at 0.007-cm and 1-cm depths in a tissue-equivalent phantom.

APPROACHES TO IN-PHANTOM DOSIMETRY USING CAVITY IONIZATION THEORY

An important segment of our research was the measurement of the dose-equivalent in a tissue-equivalent material. The dose-equivalent is equal to the absorbed dose multiplied by a quality factor. Because the quality factor for photons is usually considered to be unity, dose-equivalent and absorbed dose are considered equal in this report.

Generally, in-phantom dose measurements are based on cavity chamber theory (Burlin 1968). An extension of the theory allows measurements to be made with a small ionization chamber constructed and calibrated to measure exposure. This in-phantom exposure measurement is easily used to calculate dose in the phantom. Another method not based on exposure is the use of thermoluminescent material to make up the chamber. The absorbed dose in the material can be related to the absorbed dose in the phantom. An extrapolation chamber can also be used as a cavity ionization chamber. This type of chamber has certain advantages that make it suitable for low-energy photon dosimetry.

CALIBRATED IONIZATION CHAMBERS

An approved and often employed method of determining in-phantom dose uses ionization chambers calibrated to measure exposure (ICRU 1973). We have experienced difficulty using these types of chambers to determine the dose to the tissue from low-energy photons (Bartlett et al. 1978). In order to measure exposure, the chamber must have walls that can produce electronic equilibrium within the gas volume of the chamber. At shallow depths, however, electronic equilibrium in tissue is not achieved except for very low-energy photons; therefore, the chamber is responding to a distribution of charged particles that is not present in the surrounding region of the phantom.

Although the electronic equilibrium at a measurement depth may be sufficient to allow the use of an ionization chamber, low-energy photon measurements may still be inaccurate because of the size of the chamber. When the chamber is removed, the phantom material that had been displaced by the chamber may provide significant attenuation of a low-energy photon beam (Johns and Cunningham 1974). (The half-value layer of tissue for 15-keV photons is about

4.2 mm.) The displacement of the attenuating tissue by the chamber contributes to a perturbation correction that must be applied to the absorbed dose measurement (ICRU 1963). The perturbation corrections for the energy spectra of the photons used in this study have not been developed sufficiently for use in DEI measurements.

THERMOLUMINESCENT CAVITY CHAMBERS

Instead of a gas cavity, one could use a cavity chamber made of thermoluminescent material (Burlin 1968). This approach to in-phantom dosimetry has been used in radiation therapy measurements; however, such work usually involves photons with energies greater than 600 keV. Because the response of many thermoluminescent materials to photons with lower energies is very energy dependent, the energy spectrum of the low-energy photons must be well known so that the thermoluminescent material's response can be accurately calibrated and interpreted. The spectrum of low-energy primary and scattered photons in a phantom is very complex and varies as a function of depth in the phantom, because the material of which the phantom is made filters out various photon energies. To provide an accurate calibration of the thermoluminescent material's response for each unit of absorbed dose imparted to the material, the in-phantom energy spectrum would have to be re-created in air. Such a re-creation is impractical. We felt, therefore, that the use of thermoluminescent materials for a cavity chamber would be prohibitively difficult and would not provide the degree of accuracy desired for the photon energies of concern in this study.

EXTRAPOLATION CHAMBERS

Based on the principle of cavity ionization, an extrapolation chamber may serve as a cavity ionization chamber to allow in-phantom measurements of absorbed dose. This principle has been developed through several theories of cavity ionization (Burlin 1968; NCRP 1961). Most notable is the Bragg-Gray theory, which relates the ionization in a cavity to the absorbed dose in the material surrounding the cavity. The familiar equation to determine dose, or the energy deposited in a phantom, is:

$$E_{phantom} = S_m J_m W \qquad \text{(Eq. 5)}$$

where:

S_m is the ratio of the mass-stopping power of the phantom material to that of the cavity gas,

J_m is the ionization per unit mass of the gas in the cavity, and

W is the average energy needed to produce an ion pair in the gas.

Laurence (1937) and Spencer and Attix (1955) have refined the Bragg-Gray theory to take into account the discrete-energy-loss function of electrons and the production of energetic secondary electrons that can escape from the cavity. These refinements affect the calculation of the stopping-power ratio.

The quantity $J_m W$ is the energy deposited per unit mass of the gas. The ionization in the gas, J_m, is usually directly measured by the ionization chamber; however, when an extrapolation chamber is used, J_m is determined from a series of measurements, each one involving a progressively smaller chamber volume. The series of measurements produces data that can be extrapolated to give the ionization in an infinitesimally small cavity with zero mass of air. Multiplying the extrapolated J_m value by W yields the energy deposited in the very small cavity. This is a simplified description of the extrapolation measurements. When the approach of Spencer and Attix to cavity ionization is applied to extrapolation chambers, their calculations must be modified slightly (NCRP 1961) because their theory takes into account the size of the chamber, which varies when an extrapolation chamber is used.

The extrapolation chamber avoids many of the problems that accompany most ionization chambers. Some of its features are the following:

- It does not require electronic equilibrium because dose in air is measured rather than exposure. The ionization is extrapolated to a zero air volume so that the dose to the photon material is accurately evaluated for a specific point.
- A properly constructed extrapolation chamber can be very accurate. The uncertainty of determining the air dose has been reported to be

as low as 0.6% (ICRU 1972). This is much less than the uncertainty associated with calculating stopping powers, which is between 1% and 2% (Berger and Seltzer 1964).

- The ionization in the extrapolation chamber reflects all of the interactions that occur in the phantom material. Consequently, this type of chamber, when built into a phantom, will be extremely sensitive to the backscatter energy spectrum.

Since it was first described by Failla (1937) as a method for measuring surface and depth doses in a phantom, the extrapolation chamber has been successfully used in alpha, beta, and x-ray dosimetry (Bortner 1951; Loevinger 1953; Loevinger and Trott 1966). Although the extrapolation chamber can be extremely versatile for in-phantom measurements, the technique requires a series of measurements to obtain one value for absorbed dose. Depending on the response of the chamber to the incident radiation, the process can be very lengthy and unsuitable for routine measurements. However, we felt that this approach would enable the determination of DEI conversion factors, from which the DEI can then be calculated using routine in-air exposure measurements.

DESIGN OF A TISSUE-EQUIVALENT PHANTOM WITH AN EXTRAPOLATION CHAMBER

To measure absorbed dose (or, for photons, dose-equivalent) in a phantom, we used a large tissue-equivalent phantom with a variable-volume cavity. A drawing of the phantom is presented in Figure 1. The specifications for the extrapolation chamber are listed below.

Dimensions

Body: 30 cm x 30 cm x 15 cm.

Plug: 6.35 cm (diameter) x 20.64 cm, faced with concentric electrodes that serve either as guard rings or as a collecting electrode.

Outside guard ring: 2.22 cm wide.

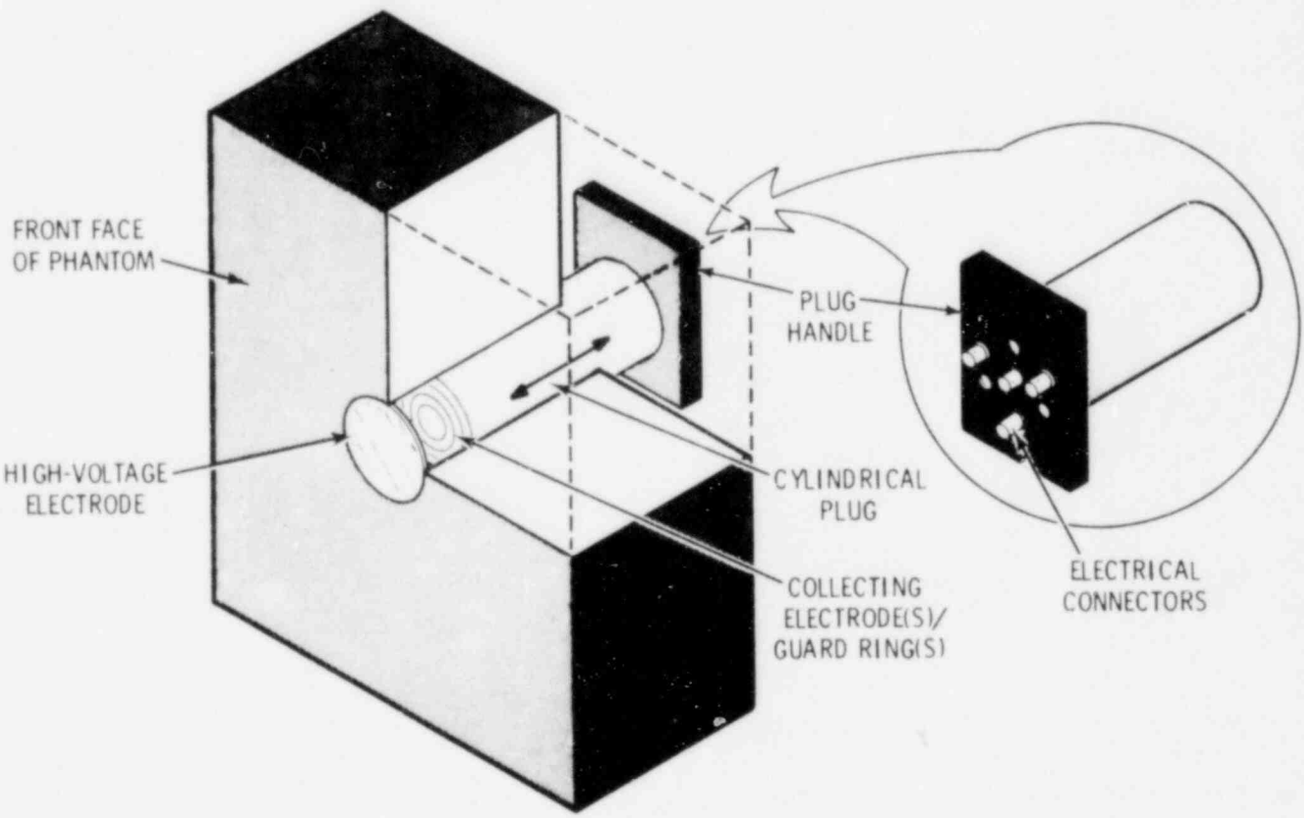

FIGURE 1. Extrapolation Chamber in a Tissue-Equivalent Phantom

Operating Conditions

Voltage potential applied to high-voltage electrode: ±100 V.

Guard ring and collecting electrode maintained at ground.

Leakage current at 100-V potential: 8×10^{-14} amp.

The design used has a cylindrical cavity between the high-voltage electrode, the center plug, and the large block of the phantom body. The volume of the cavity can be varied by moving the center plug into or out of the phantom body. The plug and the inside of the phantom body are threaded to allow precise and uniform change in the cavity volume. In the phantom used for our study, one turn of the plug changed the gap between the electrodes by 0.127 cm.

The extrapolation chamber and the phantom were made up primarily of tissue-equivalent plastic. The only other substances were a 0.01-mm coating of graphite on the interior surface of the high-voltage electrode and on the front surface of the center plug; four tungsten wires, each 0.025 mm in diameter, embedded in the plug; and four metal cable connectors on the back of the plug. The smallest possible amount of non-tissue-equivalent material was used, in order to minimize the presence of scatter that was not characteristic of tissue.

DEVELOPMENT OF A TISSUE-EQUIVALENT MATERIAL

A large number of tissue-equivalent materials has been developed to simulate many different types of tissue (White 1978b; Griffith et al. 1978). Tissues frequently simulated are muscle, adipose, bone, and lung. Many of these tissue substitutes have been developed for the medium- and high-energy photon dosimetry used in therapeutic radiology and are not suitable for use with the low photon energies used in this study. Tissue substitutes for low-energy photons must be formulated to match both the photoelectric and the Compton interactions that occur in tissue. This matching is accomplished principally by adding small amounts of trace elements to a plastic material (i.e., doping the plastic).

The development of a tissue-equivalent material was considered an important part of this study. A poor tissue substitute would introduce a bias error in the DEI conversion factors. Several methods of creating tissue substitutes have been developed (White 1978a; White 1978b). The method we used to develop the material for the phantom and the extrapolation chamber consisted of matching the mass attenuation coefficient, the mass energy absorption coefficient, and the mass-stopping power of a doped plastic for 20-keV photons and electrons to the corresponding coefficients for muscle. The muscle coefficients were based on an elemental composition of 10.2% H, 12.3% C, 3.5% N; 72.9% O; 0.08% Na; 0.02% Mg; 0.2% P; 0.5% S; and 0.3% K (ICRU 1963). Tabulated interaction coefficients and stopping-power values for this muscle formulation are available in ICRU 21 (1972) and Hubbell (1969). The interaction coefficients and the stopping power for the tissue-equivalent plastic were calculated by summing weighted coefficient values for the constituent elements. The weighting factor for each element was the weight fraction of the element in the doped plastic. This is a standard method of determining the various coefficients of mixtures (Evans 1968). The composition of the tissue-equivalent material we used is listed below.

Compound	Weight Fraction
Polyurethane Casting Resin	0.9653
$MgSO_4$	0.0075
K_2CO_3	0.0077
$NaHCO_3$	0.0029
$Ca(OH)_2$	0.0166

We felt that experimental verification of the doped plastic was necessary, to back up our calculations of the material's tissue-equivalency. The need for verification arose because of some uncertainty in the analysis of the elemental composition of polyurethane casting resin. A variation of a few tenths of a percent in the elemental composition can significantly alter the attenuation and energy absorption coefficients. This problem can be acute in tissue materials matched for low-energy photons, because the photoelectric effect is strongly dependent on the atomic number (White 1978a).

To evaluate the plastic, we measured the transmission of K-fluorescence x-rays through various thicknesses of the doped urethane. These x-ray beams are nearly monoenergetic (see Appendix A), allowing comparison of the experimental data with a muscle transmission curve derived from attenuation coefficients computed for monoenergetic photons. Muscle attenuation coefficients can be found in several references (Hubbell 1969). Because the energies of the K-fluoresence x-rays do not exactly correspond to the energies of the photons used to calculate the muscle attenuation coefficients, nonlinear interpolations were performed to determine the precise muscle attenuation coefficient for each K-fluorescence energy. Curves that compare the expected transmission to the measured transmission are presented in Appendix B.

THE EXTRAPOLATION CHAMBER

The development of a tissue-equivalent plastic was prompted in part by the desire to have a material that could be cast into both large blocks and very thin sheets. The high-voltage electrode of the extrapolation chamber was made of tissue-equivalent material about 0.007 cm thick. A 1-cm-thick block of tissue-equivalent material for measuring the deep dose-equivalent was attached to the front face of the chamber so that the high-voltage electrode would be 1 cm deep, rather than at the surface of the phantom. Because the point of measurement in this extrapolation chamber is just behind the high-voltage electrode, absorbed dose measurements were defined to be at the same depth as the high-voltage electrode.

The graphite on the front face of the cylindrical plug was divided into a series of concentric rings (see Figure 1). A narrow space was left between each ring to prevent any electrical conductivity between the rings. This isolation established each ring as a separate electrode. Each electrode was attached to a cable connector on the rear of the plug by a thin wire embedded in the plug.

The outer electrode always served as a guard ring to prevent curvature of the electric field between the collecting electrode and the high-voltage electrode (Boag 1968). This created a right cylinder, a sensitive volume that was easily quantified. The outer guard ring also served to eliminate leakage

between the high voltage electrode and the collecting electrode. All of the interior electrodes could be connected to produce one large collecting electrode, or the size of the collecting electrode could be varied by changing the number of rings connected together. Those rings not serving as part of the collecting electrode were connected with the outer guard ring to produce a larger effective guard ring. Varying the diameter of the collecting electrode allowed the sensitive volume to be changed along an axis perpendicular to the axis on which the cylindrical plug moved.

The use of an extrapolation chamber to measure absorbed dose restricts the shape of the phantom that can be used. Values for DEI are defined for a spherical phantom, but spherical curvature does not lend itself well to a parallel-electrode extrapolation chamber and is difficult to produce using a thin electrode for skin measurements. We felt that the most suitable phantom for the extrapolation design was the 30-cm x 30-cm x 15-cm phantom suggested for use as a dosimeter backing in ANSI N13.11.

IRRADIATION METHODS

Filtered and K-fluorescence x-ray sources were used to produce x-ray energies in the range of 15 to 100 keV. The filtered x-ray spectra were modified to meet the conditions specified by the NBS and defined by them as "filtered techniques" (U.S. National Bureau of Standards 1976). Use of the NBS filtered techniques, rather than K x-rays, is thought to better simulate the usual occupational exposure conditions. However, as a research tool and as a means of empirically determining conversion factors, the K-fluorescence x-rays offer the advantage of adequately simulating monoenergetic photon sources.

The DEI conversion factors presented in ANSI N13.11 apply specifically to monoenergetic photons. Therefore, K-fluorescence spectra are the most appropriate for empirical confirmation of the standard's conversion factor data. However, because both filtered and K x-ray sources are allowed by the ANSI N13.11 standard, a comparison of DEI conversion factors derived for each type of source is important.

EXPERIMENTAL DESIGN

Our x-ray sources were located in a specially designed room to minimize scattering. Ancillary electronic equipment allowed constant monitoring of the output and control systems for the x-ray sources. A detailed description of the facility and equipment is given below.

X-Ray Equipment

The configuration of the x-ray system and the supporting equipment is shown in Figure 2. The large x-ray tube has a maximum potential of 320 kVp with a 4.0- by 4.0-mm focal spot on a tungsten target. The inherent filtration is approximately equal to 2.5 mm Al. This x-ray tube is used for moderately and highly filtered NBS techniques and as an excitation source for K-fluorescence targets. To produce K x-rays, the beam is directed downward into a lead-lined beam trap made of steel. Various types of "K" radiator targets are available to produce K x-rays from 8 to 100 keV. The K x-rays are extracted

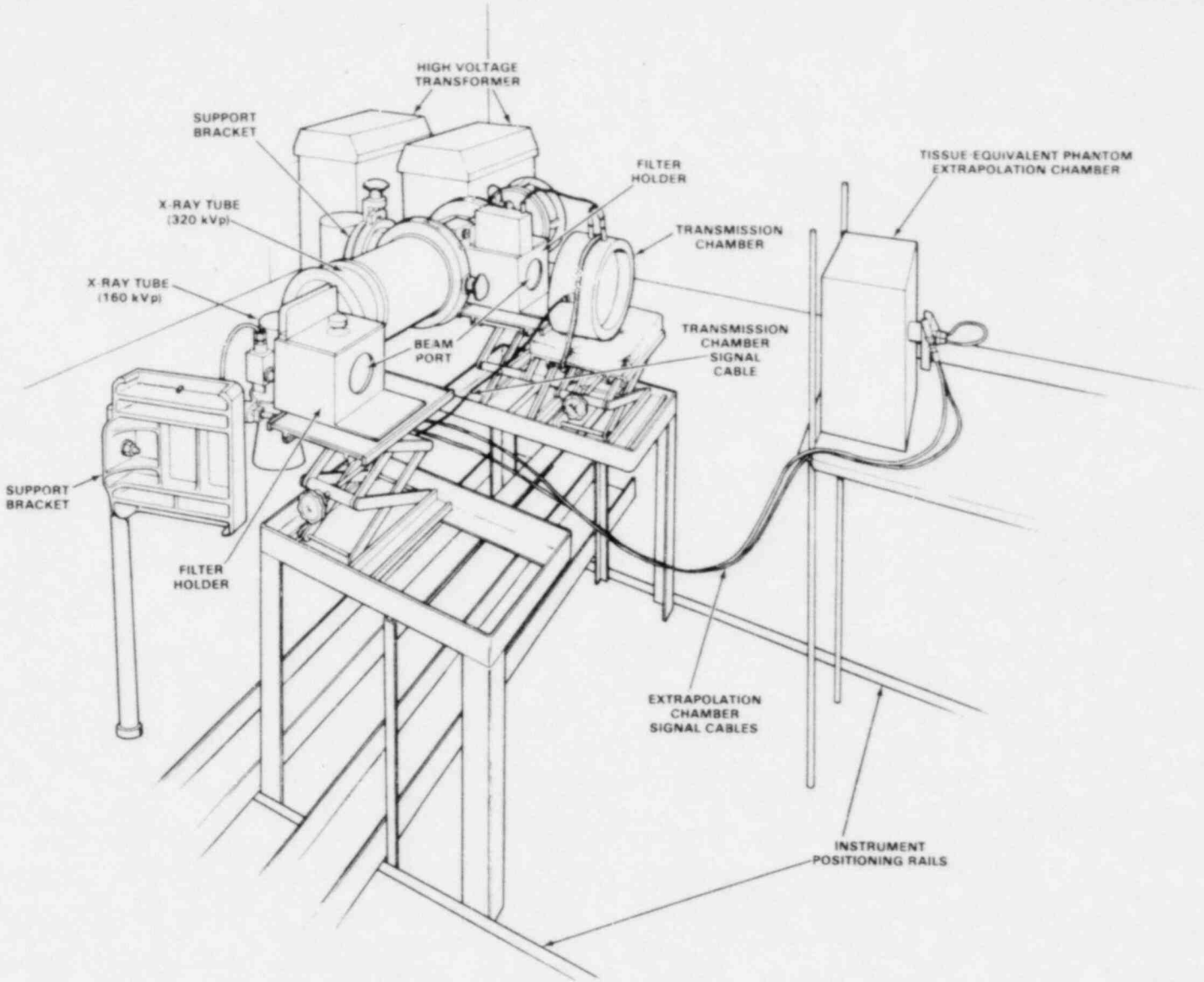

FIGURE 2. X-Ray Tube Head and Beam Control Devices

at a 90° angle to the primary beam and parallel to the filtered beams. A 160-kVp-potential x-ray tube with a beryllium window and a 3.0- by 3.0-mm focal spot on a tungsten target is available for production of lightly filtered NBS techniques.

Some of the x-ray system's support devices are also shown in Figure 2. The beam collimators (in the filter holders) are designed to produce a circular beam 30 cm in diameter at 1.0 meter from the tube target. The filter packages are equipped with appropriate thicknesses of aluminum, copper, and lead to produce the desired NBS spectra. A transmission chamber is used to provide constant monitoring of either the filtered beams or the K x-rays. The use of a transmission chamber miminizes errors introduced by fluctuations in the current. Each x-ray technique is calibrated in terms of roentgens (at the point of interest) per coulombs delivered to the transmission chamber (the R/C factor). Steel-rail alignment devices are available for exact tube-target-to-detector and lateral positioning. Laser devices are used for reference alignment. Measurements are made to determine the influence of backscatter into the transmission chamber from any experimental arrangement.

Determination of Beam Quality

Many beam parameters must be measured in order to accurately assess the quality of an x-ray spectrum. The monoenergetic nature of the K x-ray beam simplifies these measurements. Even so, the K x-ray beam can have two to four different energy peaks that can contribute significantly to the exposure and therefore should be characterized (Storm, Lier and Israel 1974). The important parameters in determining beam quality are discussed below.

The maximum energy of the x-ray spectrum is determined by the applied potential. Slight variations in the applied potential (i.e., a change of a few percent) can cause significant changes in the exposure rate and the energy distribution (Bartlett et al. 1978). Therefore, we used a calibrated resistor chain to directly monitor tube voltage. The resistor chain was calibrated by comparing the measured voltage to the excitation thresholds of characteristic radiation (Bartlett et al. 1978). The voltages were monitored and controlled to within a few tenths of a percent.

The effective energy of the beam was determined by half-value layer (HVL) measurements and spectroscopic analysis. The experimental arrangement for the HVL measurements was similar to that published elsewhere (Johns and Cunningham 1974). The measured HVLs and the beam homogeneity factors for the NBS and K x-ray techniques are shown in Appendix A. Spectroscopic measurements were made using a low-energy Ge(Li) detector interfaced with a multichannel analyzer and corrected for detector efficiency (see Appendix A).

Beam uniformity was an important consideration (Bartlett et al. 1978). The "heel" effect (Johns and Cunningham 1974) is not the only cause of a non-uniform beam. Irregularities in the tube target may produce "hot spots" in the beam. Therefore, beam mapping using a precision instrument (i.e., an inter-comparison ionization chamber) is necessary to measure 1% to 2% variations in the beam. A typical beam map is shown in Figure 3. Small "hot spots" in the beam were taken into consideration when the detectors were positioned. Exact, reproducible positioning of detectors is important if accurate and repeatable measurements are needed.

The x-ray exposure room was large enough to allow a distance of 9.0 m between the tube target and the first primary barrier. The filtered beams

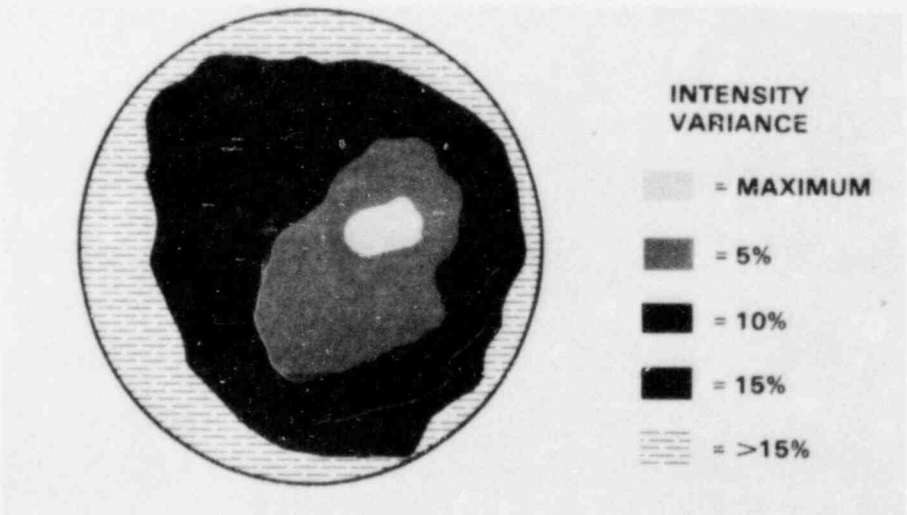

FIGURE 3. Typical Beam Uniformity Map (320 kVp, filtered technique, 28-cm diameter)

were approximately 1.0 m from the floor, and the K x-ray beam was 0.6 m from the floor. All support devices, including the holders for the lead collimators, were constructed of aluminum to reduce scatter.

MEASUREMENT TECHNIQUES AND NBS INTERCOMPARISONS

The NBS routinely calibrates intercomparison ion chambers for all of the filtered techniques used in this study. In addition, electronic equipment (e.g., electrometers and voltmeters) routinely receives an NBS-traceable calibration. Appropriate instrument, temperature, pressure, and calibration factors are applied to all roentgen measurements.

Primary roentgen measurements were made for this study using free-air ionization chambers rather than intercomparison chambers. The use of free-air ionization chambers has been well documented and will not be discussed here (U.S. National Bureau of Standards 1957; Attix 1961; Victoreen Instrument Company [No date]). These chambers have two advantages. First, the chamber aperture acts as a more exact reference point in space (Attix 1961) than does a standard cyclindrical ionization chamber (Johns and Cunningham 1974). Second, the chamber can be used to determine calibration factors for K x-rays. (The NBS does not have K x-ray sources available for intercomparison measurements.)

DETERMINATION OF DEI CONVERSION FACTORS

Conversion factors for shallow and deep DEIs were determined for all of the basic x-ray beams produced at the PNL calibration laboratory (see Appendix A). In accordance with paragraph 2.4 in ANSI N13.11, the shallow and deep DEIs were equated with the dose-equivalent measured at 0.007-cm and 1.0-cm depths, respectively. Determining the DEI conversion factors involved two tasks, in-air exposure calibrations and in-phantom dose-equivalent measurements.

IN-AIR EXPOSURE CALIBRATIONS

In-air exposure calibrations were made for each x-ray beam using a free-air ionization chamber. The chamber was situated in the beam to determine the exposure at a point a specific distance from the x-ray source. The beam diameter at this point was 30 cm for all x-ray energies. For filtered x-rays, this point was along the central axis of the beam and 100 cm from the source. For K-fluorescence x-rays, two calibration points were located along the central axis at 50 and 100 cm from the source. By using two calibration points, we could confirm the relative geometric independence of the DEI conversion factors for the K-fluorescence beams.

As described in the previous section, each beam was monitored with a transmission chamber to account for variations in the x-ray machine's output. The coulombs collected in this chamber during calibration were divided into the roentgens measured with the free-air ionization chamber, to obtain an R/C factor. For later irradiations, the number of coulombs collected in the transmission chamber could be used with the R/C factor to calculate the number of roentgens produced at the calibration point. The R/C factors for the x-ray beams are presented in Appendix C.

MEASUREMENT OF DOSE-EQUIVALENT

All dose-equivalent measurements were made using the tissue-equivalent phantom and extrapolation chamber. Shallow dose-equivalents were measured with the high-voltage electrode serving as the 0.007-cm layer of tissue. Deep

measurements were made with a 1-cm-thick buildup plate of tissue-equivalent material attached to the front of the phantom. The dose value measured using the extrapolation chamber is defined for a point immediately behind the high-voltage electrode; therefore, the depth of the electrode determined the depth of the dose-equivalent measurement.

The phantom was centered along the central axis of the beam. A laser assured proper alignment. The high-voltage electrode was centered on the in-air calibration point so that the DEI measurement and the exposure measurement were made at the same point. The advantage of this arrangement was that the phantom did not have to be repositioned for the shallow and deep dose measurements. The only difference between the shallow and deep measurements was the presence of the 1-cm-thick plate that became the surface of the phantom extrapolation chamber for deep measurements. With the buildup plate in place, the distance from the source to the plate surface was 1 cm less than the distance to the high-voltage electrode, which was either 50 or 100 cm from the source, depending on the intensity of the x-ray technique involved.

Knowledge of the ionization in an infinitesimally small air cavity was central to the calculation of dose-equivalent indices. This information was obtained for each x-ray energy and depth from a series of measurements in the extrapolation chamber. Ionization measurements were made for progressively smaller gaps between the high-voltage electrode and the collecting electrode. An electrometer was used to measure collected charge. For each gap size, measurements were made with the high-voltage electrode at +100 V and -100 V with respect to the collecting electrode, which was always kept at ground potential. Three measurements were made at each polarity of the high-voltage electrode. The variations among the three measurements were found to be less than 0.5%. For each gap size, the absolute values of the ionizations obtained at each polarity were averaged. The average ionization measured at each gap size was plotted against the gap distance. The plot resulting from this series of extrapolation measurements produced a straight line for gaps of less than 5.8 mm. The slope of this line (in C/in.) represented the ionization in an infinitesimally small cavity (Bortner 1951; Failla 1937) and was determined from a stepwise-regression computer program which calculated the best line that

passed through at least the three smallest gaps. Typically, five gaps fell along the best straight line. The individual slopes determined for each x-ray energy and depth are presented in Appendix D.

CALCULATION OF CONVERSION FACTORS

Calculation of the dose-equivalent was based on the theoretical Bragg-Gray equation presented earlier (Equation 5). The use of the equation in this study produced the dose-equivalent delivered to the phantom per coulomb of charge collected in the transmission chamber. Since the exposure calibration factor gave the exposure in air per coulomb collected in the transmission chamber, the DEI conversion factor was obtained from the ratio of the dose-equivalent per coulomb to the calibration factor. The actual formula, incorporating the Bragg-Gray equation, is presented below.

$$\text{DEI conversion factor } \left(\frac{\text{rem}}{\text{R}}\right) = \frac{\frac{E \cdot W \cdot S \cdot QF}{A \cdot T}\, k}{X} \qquad \text{(Eq. 6)}$$

where:

E is the extrapolated ionization or slope of the line, in C/in.

W is the average energy needed to produce an ion pair (ip), in eV/ip

S is the ratio of the mass-stopping power of tissue to that of air

QF is the quality factor (assumed to be unity)

A is the area of the collecting electrode (2.074 $in.^2$)

T is the number of coulombs collected in the transmission chamber for the ionization E

X is the calibration factor, in R/C, and

k is the units conversion constant, in $(in.^3 \cdot rads \cdot ip)/(C \cdot eV)$.

The average energy needed to produce an ion pair, W, is discussed in ICRU 31 (1979). The value traditionally recommended for W had been 33.73 eV/ion pair. In ICRU 31, a new value, 33.85 eV/ion pair, was recommended. This

new value was defined for dry air and was adapted into the formula we used for the conversion factor. We later applied a correction factor of 1.003 (ICRU 1979) to this value to account for the relative humidity in our laboratory, which ranged between 30% and 40%. Because we expected electrons of relatively low energies in this study, an additional correction for W was made. This correction was adopted from Waibel and Grosswendt (1978) and ICRU (1979), with the new W value for dry air substituted into their correction formula. The value for W used in this study was calculated for 10-keV electrons. When corrected for humidity and energy, this value was 34.1 eV/ion pair.

As E is equal to the slope of the extrapolated data plot and is expressed in C/in., the quantity E/A in Equation 6 represents the ionization per cubic inch in an infinitesimally small cavity. The quantity E•W•S/A is the Bragg-Gray expression for the amount of energy per unit volume deposited in air. The density of air was used to convert from volume to mass of air per cubic inch and was one component of the constant k. Because the transmission chamber always monitored the x-ray beam, the energy deposited in the phantom per coulomb collected in the transmission chamber was represented as (E•W•S)/(A•T).

The quantity S is the ratio of the mass-stopping power of tissue to that of air. The mass-stopping power for each compound was calculated from equations presented by Berger and Seltzer (1964). Since our study dealt with photons with energies less than 200 keV, the energy of the electrons produced in the phantom was low enough so that the stopping-power number did not have to be corrected for the density effect (Berger and Seltzer 1966). Another correction that is sometimes considered results from application of the Spencer-Attix theory (1955). This theory corrects for the production of energetic secondary electrons that do not deposit their entire energy in the air cavity. The correction is dependent on the size of the cavity and the energy of the electrons. The theory is applicable when the initial energy of the primary electrons is between 300 keV and several MeV (Burlin 1968). Since the photon energies used in this study generated electrons with energies less than 300 keV, the Spencer-Attix theory was not applied.

The mass-stopping powers for air and tissue were each a weighted average stopping power obtained by weighting the mass-stopping power for the initial

energy of the photoelectrons, and the average energy of Compton electrons produced from the x-ray interaction. The weighting factor for each mass-stopping power was the ratio of the interaction coefficients for each process (photoelectric and Compton) to the total interaction coefficient for the x-ray energy. The x-ray energy for K-fluorescence x-rays was considered equal to the K x-ray energy of the K irradiator. The effective energy assigned to the spectrum of x-rays produced by the NBS filtered technique was equal to the energy of a monoenergetic photon with the same half-value layer as the x-ray spectrum. The effective energies determined by NBS for their x-ray techniques were used. Tabulated ratios for mass-stopping power are presented in Appendix E.

The units conversion constant, k, is equal to 4.719×10^6 $(in.^3 \cdot rads \cdot ip)/(C \cdot eV)$. It includes the conversion of cubic inches to cubic centimers; the elementary charge, coulombs per ion pair; the mass of air at standard temperature and pressure; the conversion of electron volts to ergs; and the conversion of ergs per gram to rads.

All measurements of the DEI conversion factor were repeated at least once. Some were repeated a second time for a better estimate of the experimental variation. The average DEI conversion factors are presented in Appendix D. Plots comparing the average DEI conversion factors measured in this study with the factors listed in ANSI N13.11 are presented in Figures 4 through 9.

DISCUSSION OF RESULTS

Several points are interesting. Above about 50 keV, the DEI conversion factors for the nearly monoenergetic K x-rays were significantly higher than the conversion factors for the filtered x-rays. This was evident for both deep and shallow measurements (Figures 4 and 5). At energies less than 50 keV, the conversion factors for K x-rays were lower than those for the filtered x-rays. The probable reason is the relatively wide energy spectra associated with the filtered x-ray techniques. These wide spectra are specified in terms of effective energy. The usual method of determining effective energy is to determine a monoenergetic photon energy that has the same half-value layer in aluminum as the heteroenergetic filtered beam. For wide spectra, this method

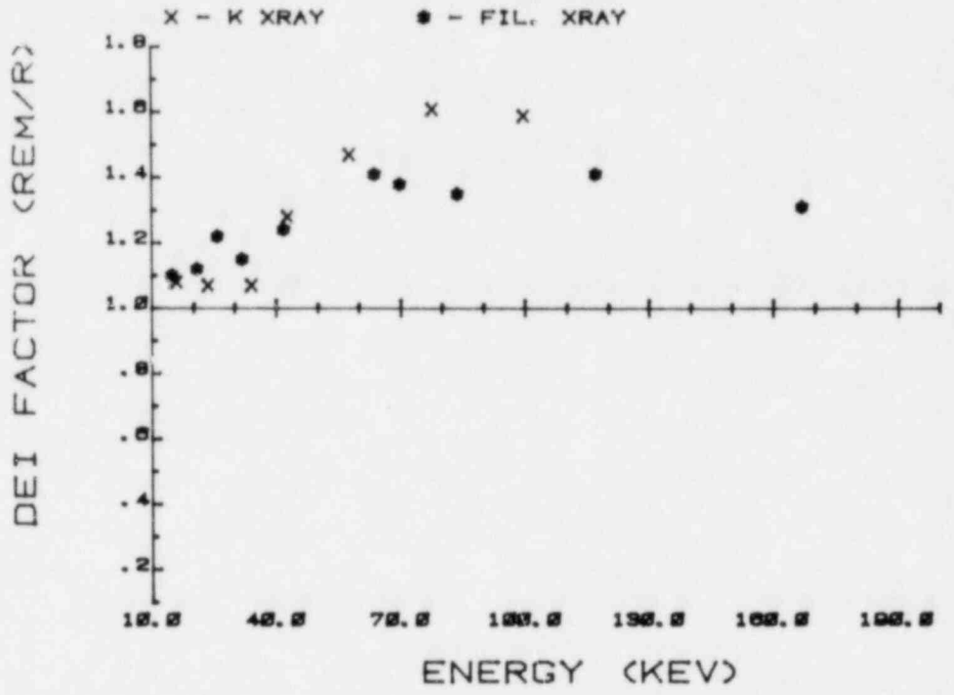

FIGURE 4. Comparison of K X-Ray and Filtered X-Ray Conversion Factors - Shallow DEI

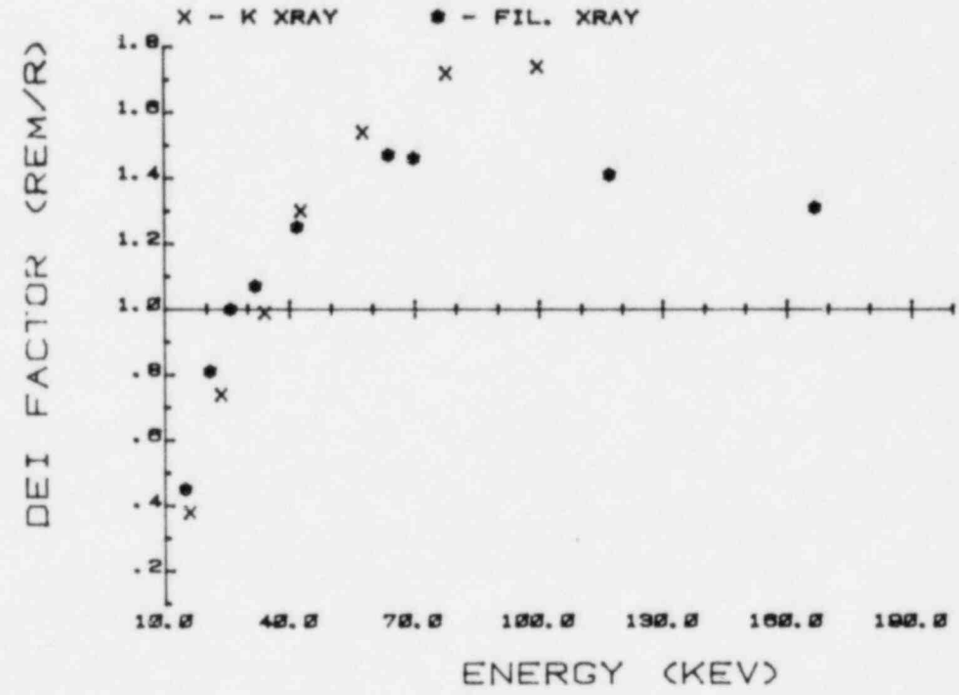

FIGURE 5. Comparison of K X-Ray and Filtered X-Ray Conversion Factors - Deep DEI

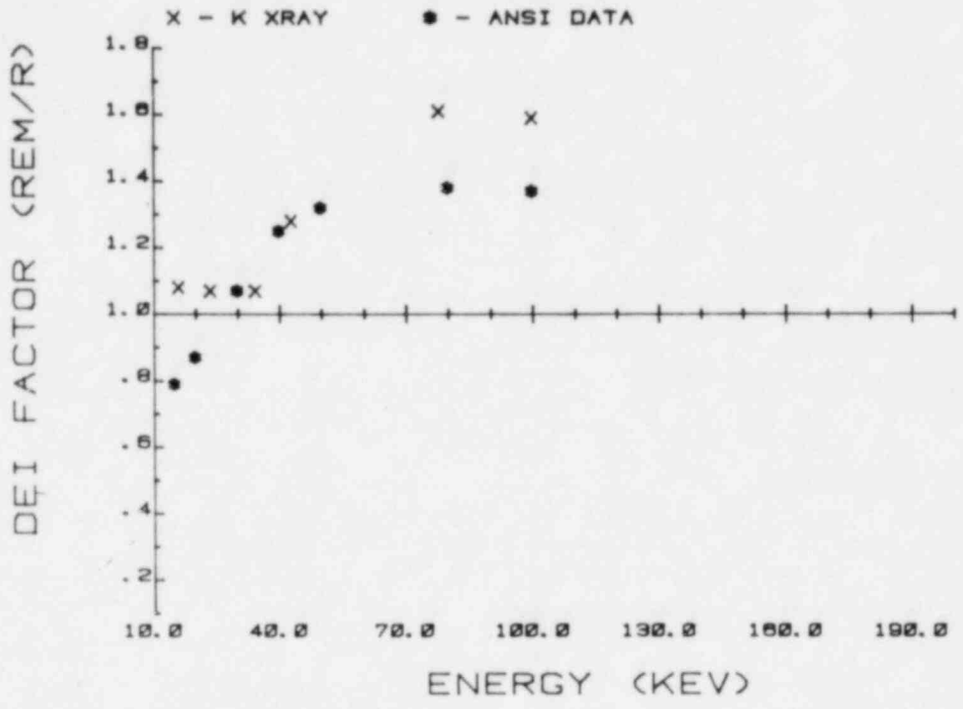

FIGURE 6. Comparison of K X-Ray and ANSI Conversion Factors - Shallow DEI

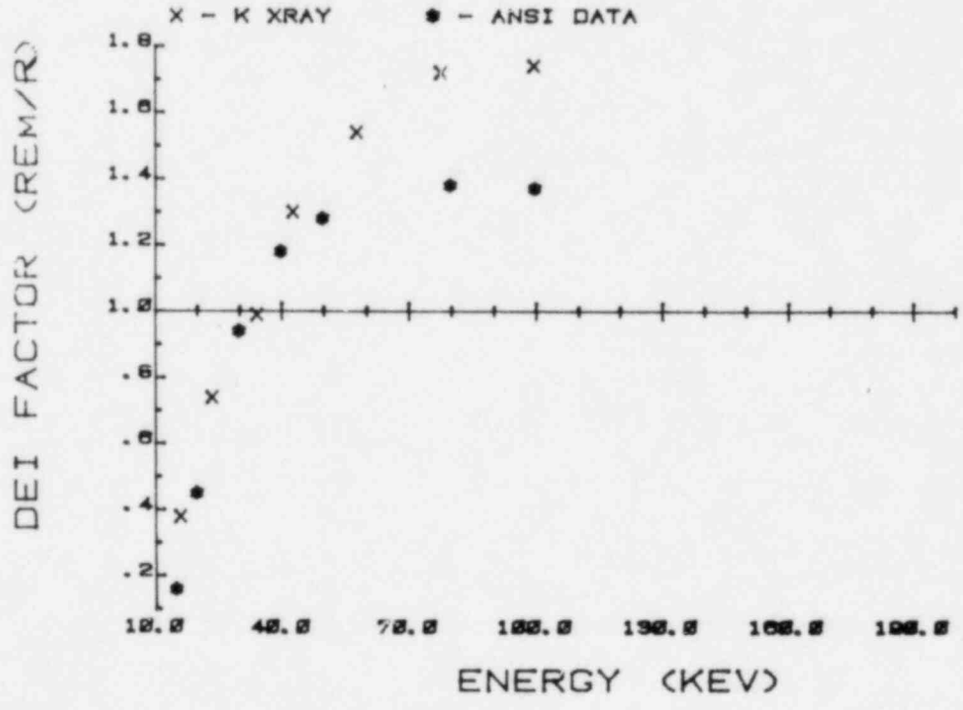

FIGURE 7. Comparison of K X-Ray and ANSI Conversion Factors - Deep DEI

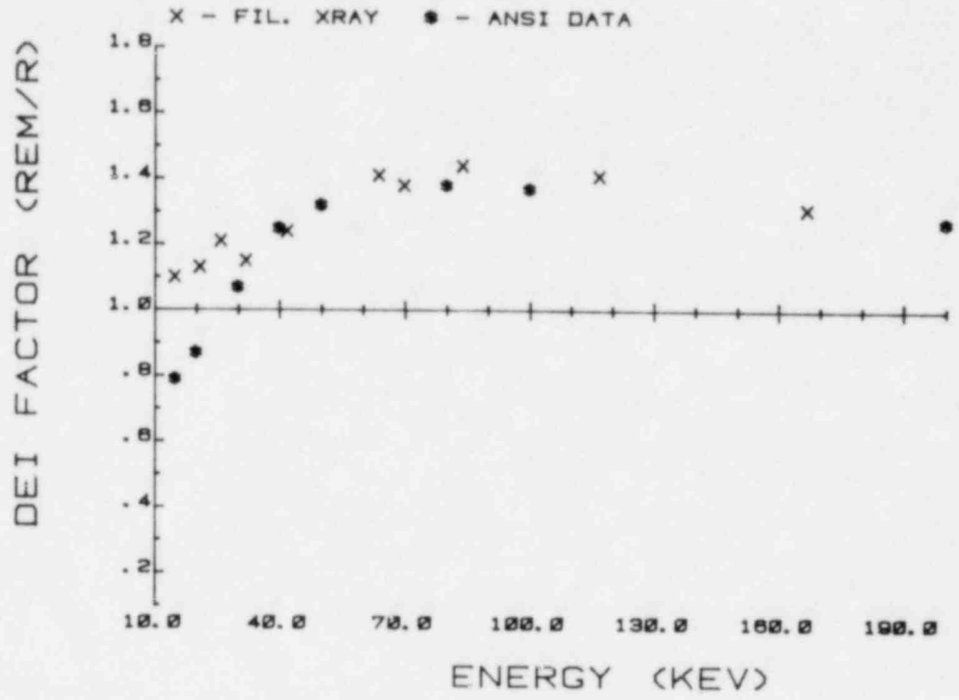

FIGURE 8. Comparison of Filtered X-Ray and ANSI Conversion Factors - Shallow DEI

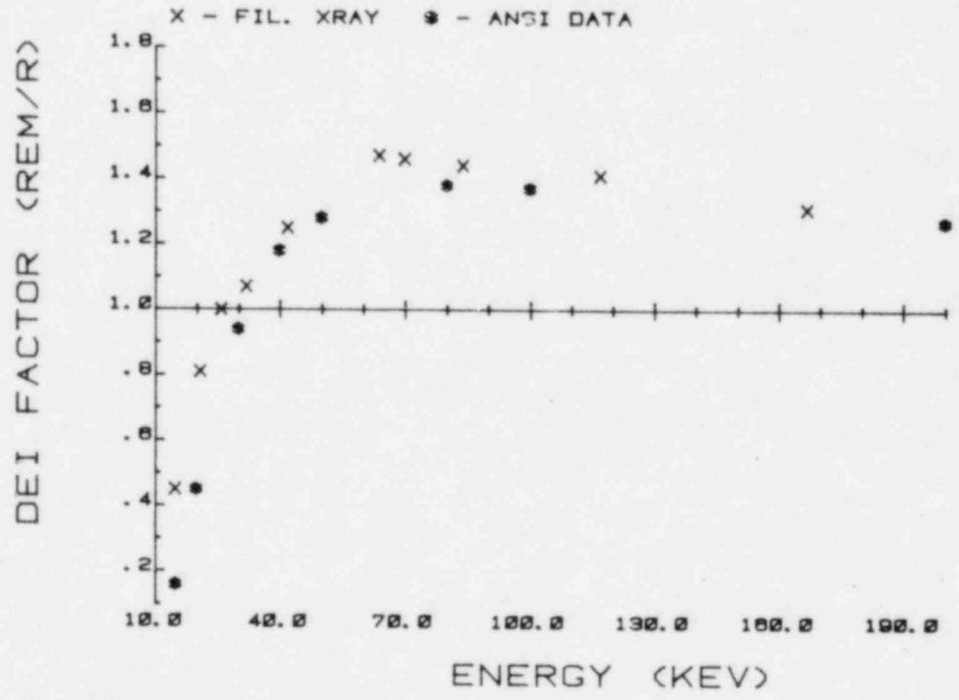

FIGURE 9. Comparison of Filtered X-Ray and ANSI Conversion Factors - Deep DEI

may be inappropriate; a spectroscopic specification of low-energy x-ray beams, such as the average energy of the spectrum, the medium energy of the spectrum, or the mode of the spectrum, might be more useful.

The DEI conversion factors for the K x-rays were very different from the conversion factors in ANSI N13.11, which are also for monoenergetic photon beams. The difference is most notable above 50 keV (Figures 6 and 7). An explanation might be found in one source of the ANSI conversion factors. For the shallow DEI for energies between 40 and 100 keV, the standards committee referred to Publication 21 of the International Commission on Radiological Protection (1969). This publication presented a graph of backscatter factors compiled from both monoenergetic and heteroenergetic data originally published by H. J. Delafield (1963). Delafield had used filtered x-ray spectra to obtain backscatter factors for photon energies less than 200 keV. (The use of these backscatter factors to derive the ANSI conversion factors may also account for the similarity between the ANSI factors and our derived filtered factors for the shallow DEI.) The degree of difference between the ANSI factors and the monoenergetic K x-ray factors indicates that further investigation is warranted before the ANSI N13.11 standard is adopted.

The DEI conversion factors for the 23.7- and 34.3-keV K x-rays were determined at source-to-phantom distances of 50 and 100 cm, to check the sensitivity of the conversion factors to distance from the source. The deep DEI conversion factors for the 23.7-keV x-ray at 50 and 100 cm were 0.74 and 0.73, respectively. The shallow DEI conversion factors for the 34.3-keV x-ray at 50 and 100 cm were 1.07 and 1.13, respectively. The difference between the latter two factors is only 5.3%, which is probably not statistically significant.

REFERENCES

American National Standards Institute. 1978. Draft American National Standard Criteria for Testing Personnel Dosimetry Performance. ANSI N13.11, New York, New York.

Attix, F. H. 1961. Electronic Equilibrium in Free-Air Chambers and a Proposed New Chamber Design. NRL Report 5646, U.S. Naval Research Laboratory, Washington, D.C.

Bartlett, W. T., J. P. Holland, C. D. Hooker, O. R. Mulhern and D. M. Fleming. 1978. "The Use of a Phantom in Personnel Dosimetry Photon Calibrations." In: International Symposium on National and International Standardization in Radiation Dosimetry, International Atomic Energy Association, Vienna.

Berger, M. J., and S. M. Seltzer. 1964. Tables of Energy Losses and Ranges of Electrons and Positrons. NASA-SP-3012, National Aeronautics and Space Administration, Washington, D.C.

Berger, M. J., and S. M. Seltzer. 1966. Additional Stopping Power and Range Tables of Protons, Mesons and Electrons. NASA-SP-3036, National Aeronautics and Space Administration, Washington, D.C.

Boag, J. W. 1968. "Ionization Chambers." In: Instrumentation, Vol. 2 of Radiation Dosimetry, eds. F. H. Attix and W. C. Roesch. 2nd ed. Academic Press, New York, New York.

Bortner, T. E. 1951. "An Extrapolation Chamber: Construction and Use." Nucleonics 9(3):40.

Burlin, T. E. 1968. "Cavity Chamber Theory in Radiation Dosimetry." In: Fundamentals, Vol. 1 of Radiation Dosimetry, eds. F. H. Attix and W. C. Roesch. 2nd ed. Academic Press, New York, New York.

Delafield, H. J. 1963. Gamma Ray Exposure Measurements in a Man Phantom Related to Personnel Film Dosimetry. AERE-R 4430, Atomic Energy Research Establishment, Health Physics and Medical Division, Harwell, Berkshire, England.

Evans, R. D. 1968. "X-Ray and Gamma-Ray Interactions." In: Fundamentals, Vol. 1 of Radiation Dosimetry, eds. F. H. Attix and W. C. Roesch. 2nd ed. Academic Press, New York, New York.

Failla, G. 1937. "The Measurement of Tissue Dose in Terms of the Same Unit for All Ionizing Radiations." Radiology 29:202.

Friem, J. O., and A. Feldman. 1978. "Communications." Med. Phys. 5:454.

Griffith, R. V., P. N. Dean, A. L. Anderson and J. C. Fisher. 1978. Fabrication of a Tissue Equivalent Torso Phantom for Intercalibration of In-Vivo Transuranic-Nuclide Counting Facilities. UCRL-80343, Lawrence Livermore Laboratory, Livermore, California.

Hubbell, H. J. 1969. Photon Cross Sections, Attenuation Coefficients and Energy Absorption Coefficients from 10 keV to 100 GeV. NSRDC-NBS 29, U.S. National Bureau of Standards, Washington, D.C.

International Commision on Radiation Units and Measurements (ICRU). 1963. Physical Aspects of Irradiation. ICRU 10b, Washington, D.C.

International Commision on Radiation Units and Measurements (ICRU). 1971. Radiation Quantities and Units. ICRU 19, Washington, D.C.

International Commision on Radiation Units and Measurements (ICRU). 1972. Radiation Dosimetry: Electrons with Initial Energies Between 1 and 50 MeV. ICRU 21, Washington, D.C.

International Commision on Radiation Units and Measurements (ICRU). 1973. Measurement of Absorbed Dose in a Phantom Irradiated by a Single Beam of X or Gamma Rays. ICRU 23, Washington, D.C.

International Commision on Radiation Units and Measurements (ICRU). 1976. Conceptual Basis for the Determination of Dose Equivalent. ICRU 25, Washington, D.C.

International Commision on Radiation Units and Measurements (ICRU). 1979. Average Energy to Produce an Ion Pair. ICRU 31, Washington, D.C.

International Commission on Radiological Protection. 1969. Data for Protection Against Ionizing Raidation from External Sources: Supplement to ICRP Publication 15. ICRP Publication 21, Pergamon Press, Elmsford, New York.

Johns, H. E., and J. R. Cunningham. 1974. The Physics of Radiology. Charles C. Thomas, Inc., Springfield, Illinois.

Laurence, G. C. 1937. "The Measurement of Extra Hard X-Rays and Gamma-Rays in Roentgens." Can J. Res. A15:67.

Loevinger, R. 1953. "Extrapolation Chamber for the Measurement of Beta Sources." Rev. Sci. Inst. 24:907.

Loevinger, R., and N. G. Trott. 1966. "Design and Operation of an Expolation Chamber with Removable Electrodes." Int. J. Appl. Rad. Isotopes 17:103.

National Council on Radiation Protection and Measurements (NCRP). 1961. Stopping Powers for Use with Cavity Ionization Chambers. NCRP 27, Washington, D.C.

Spencer, L. V., and F. H. Attix. 1955. "A Theory of Cavity Ionization." Rad. Res. 3:329.

Storm, E., D. W. Lier, and H. I. Israel. 1974. "Photon Sources for Instrument Calibration." Health Phys. 26:179.

U.S. Department of Health, Education and Welfare, Public Health Service. 1970. Radiological Health Handbook. U.S. Government Printing Office, Washington, D.C.

U.S. National Bureau of Standards. 1957. Design of Free-Air Ionization Chambers. Handbook 64, U.S. Government Printing Office, Washington, D.C.

U.S. National Bureau of Standards. 1976. Calibration and Test Services of the National Bureau of Standards. NBS Special Publication 250, U.S. Government Printing Office, Washington, D.C.

Victoreen Instrument Company. (No date). Instruction Manual for Model 481 Free-Air Ionization Chamber. Cleveland, Ohio.

Waibel, E., and B. Grosswendt. 1978. "Determination of W-Values and Backscatter Coefficients for Slow Electrons in Air." Rad. Res. 76:241.

White, D. R. 1978a. "Effective Atomic Numbers in the Formulation of Tissue Substitute Materials for Photons." Rad. Res. 76:23.

White, D. R. 1978b. "Tissue Substitutes in Experimental Radiation Physics." Med. Phys. 5:467.

APPENDIX A

HALF-VALUE LAYER AND SPECTROSCOPIC DATA

APPENDIX A

HALF-VALUE LAYER AND SPECTROSCOPIC DATA

The NBS and PNL filtered x-ray techniques used in this study are compared in Table A.1. The effective x-ray energy used by PNL was the same as that specified by NBS. Using a weighted averaging technique (ANSI N13.11) or deriving an effective energy by comparison to standard curves (U.S. Department of Health, Education and Welfare 1970) would yield slightly different effective energies and cause slight variations in the DEI function for filtered techniques.

The main purpose of this study was to confirm monoenergetic conversion factors; therefore, no attempt was made to evaluate the most appropriate method of determining the effective energies of filtered techniques. The inherent filtration of the x-ray tube used for "L" techniques was approximately 1.0 mm of Be, and the inherent filtration for other filtered techniques was 2.5 mm of Al equivalent. The filtration added at PNL was varied to achieve the first half-value layer and homogeneity factors specified by NBS. Uncorrected x-ray spectra for filtered techniques are shown in Figures A.1 through A.10. Because of the broad nature of these spectra, the importance of the energy dependence of backscatter and absorption is less appparent in the DEI measurements.

The K x-ray techniques used at PNL are shown in Table A.2. The voltage was adjusted for each technique to optimize the relationship between K X-ray output and Compton scatter. The assigned energy refers to the energy used for DEI calculations and graphs. Figures A.11 through A.16 show uncorrected spectra for the K x-ray beams. It is important to note that very little of the beam is due to Compton or other scattered photons. The spectra emphasize the usefulness of the K x-ray in simulating monoenergetic photon sources.

Standard spectra for ^{241}Am are presented in Figure A.17 and A.18 for comparison.

TABLE A.1. Comparison of NBS and PNL Filtered X-Ray Techniques

Technique Designation	kVp (NBS & PNL)	Effective keV (NBS)	Added Filtration, mm (NBS)	First HVL, mm (NBS)	Homogeneity Coefficient (NBS)	First HVL, mm (PNL)	Homogeneity Coefficient (PNL)
L-G	30	15	0.5 Al	0.36 Al	0.64	0.37	0.68
L-I	50	21	1.0 Al	1.02 Al	0.66	1.04	0.70
L-K	75	26	1.5 Al	1.86 Al	0.63	1.81	0.65
MFC	60	32	2.5 Al	2.8 Al	0.79	2.79 Al	0.79
MFE	76	34.5	2.51 Al	3.4 Al	0.74	3.39 Al	0.74
MFG	100	42	3.5 Al	5.1 Al	0.73	5.03 Al	0.73
MFI	150	64	3.49 Al 0.25 Cu	10 Al	0.89	10.25 Al	0.89
MFK	200	84	3.49 Al 0.5 Cu	1.3 Cu	0.92	13.2 Al	0.92
HFE	100	70	2.5 Al 0.5 Pb	11.20 Al	--	11.20 Al	--
HFG	150	117	2.5 Al 1.51 Sn 4.0 Cu	16.96 Al	--	16.81 Al	--
HFI	200	167	2.47 Al 0.77 Pb 4.16 Sn 0.6 Cu	19.60 Al	--	19.61 Al	--

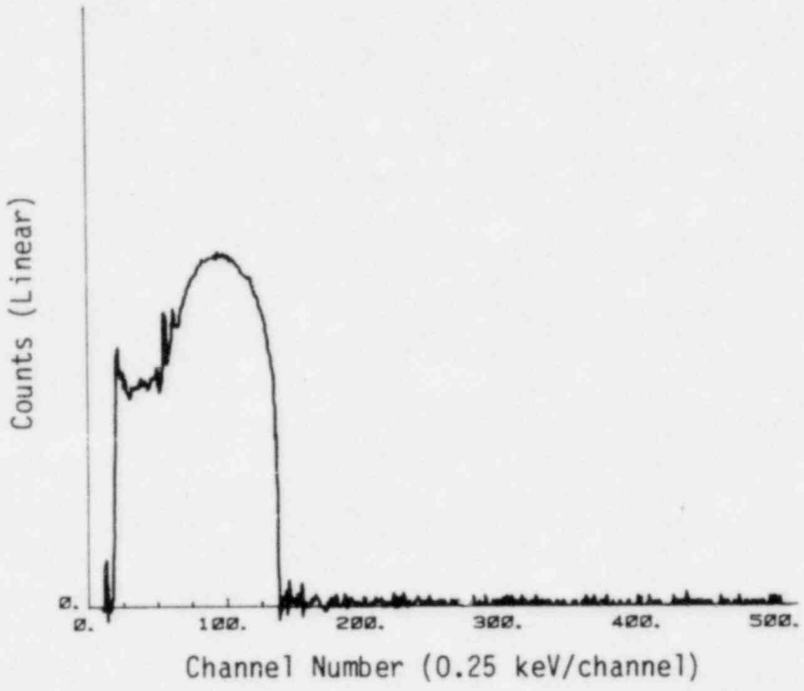

FIGURE A.1. Spectrum from NBS Technique LG

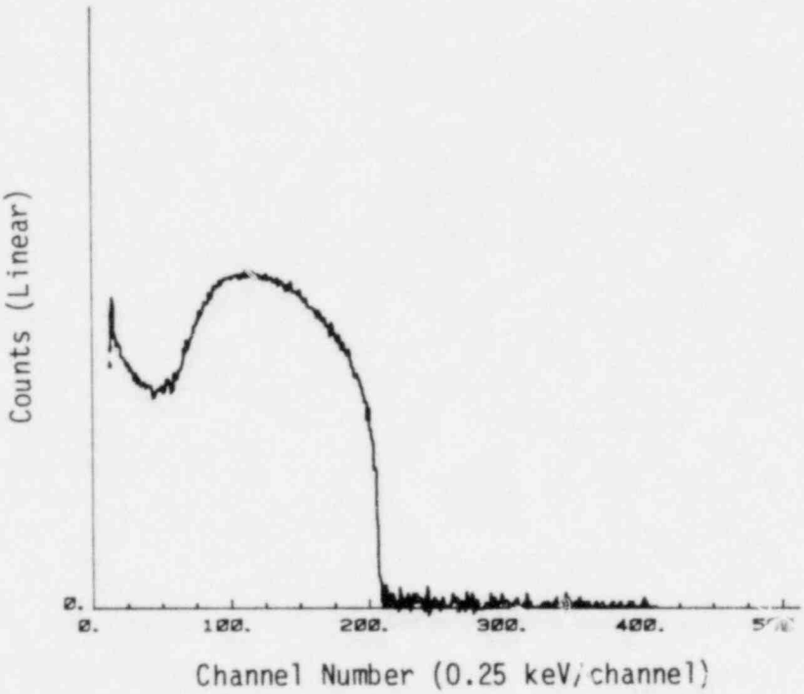

FIGURE A.2. Spectrum from NBS Technique LI

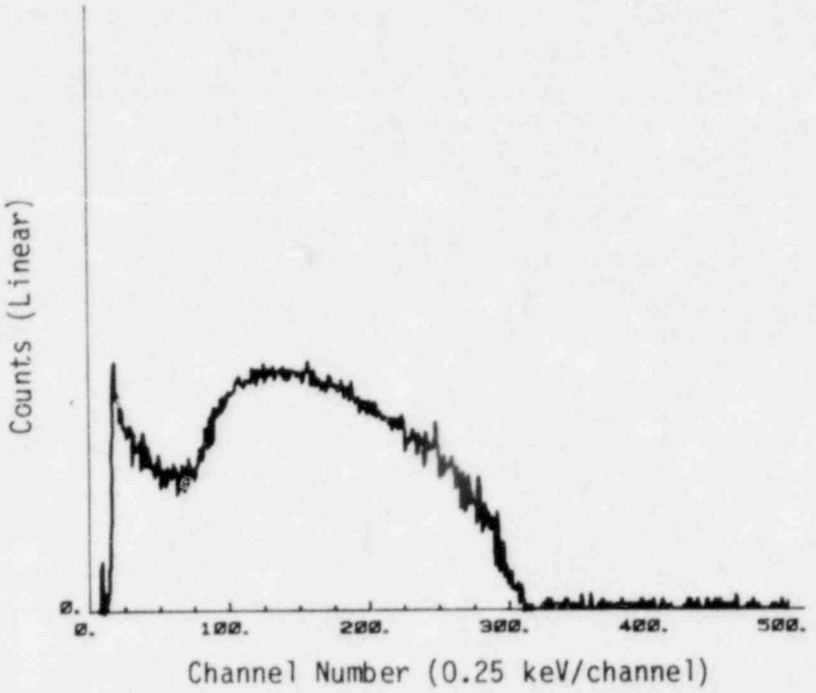

FIGURE A.3. Spectrum from NBS Technique LK

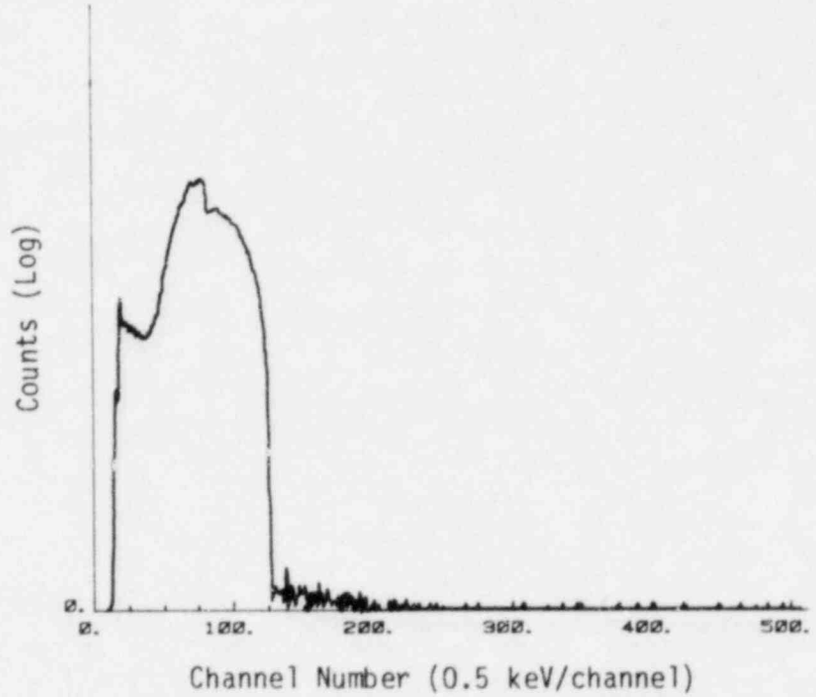

FIGURE A.4. Spectrum from NBS Technique MFC

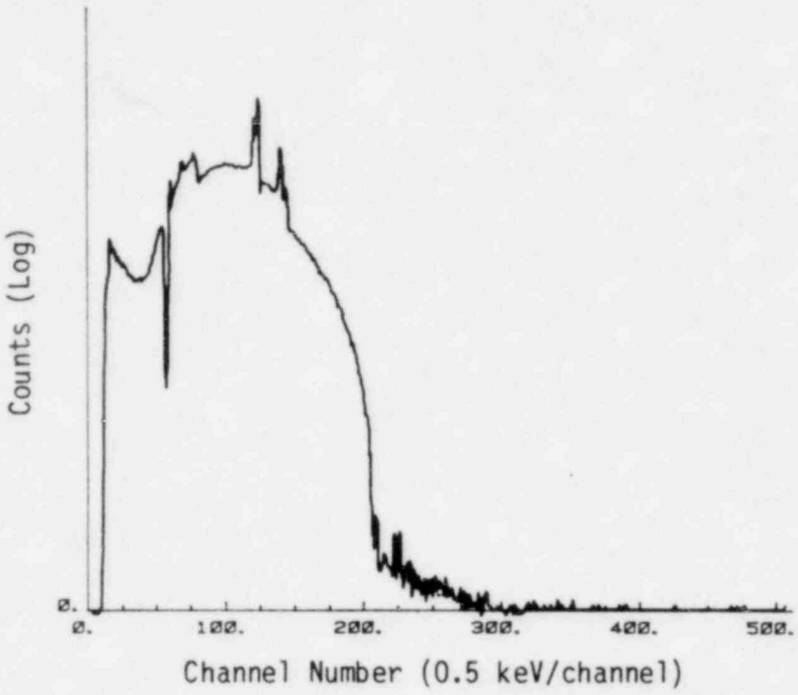

FIGURE A.5. Spectrum from NBS Technique MFG

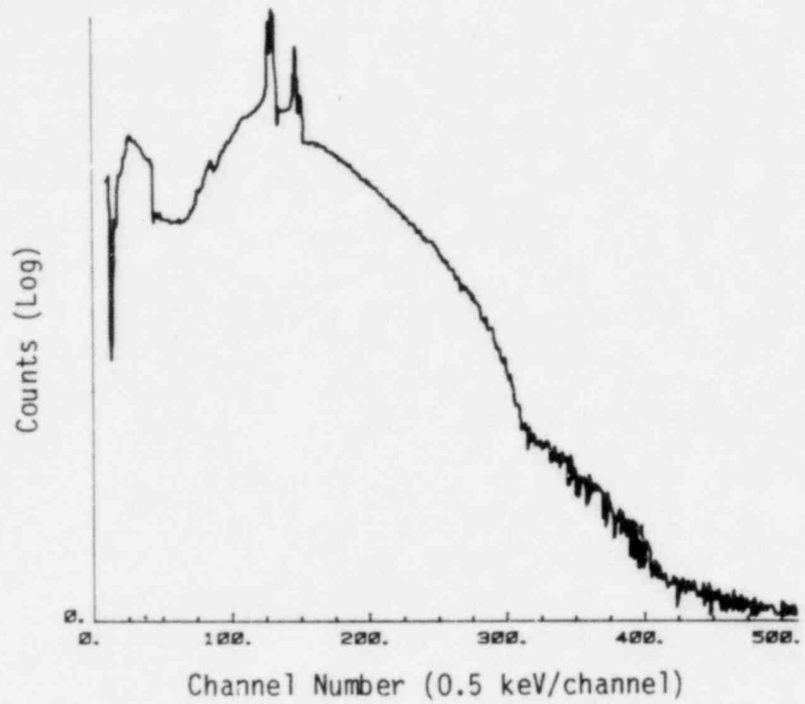

FIGURE A.6. Spectrum from NBS Technique MFI

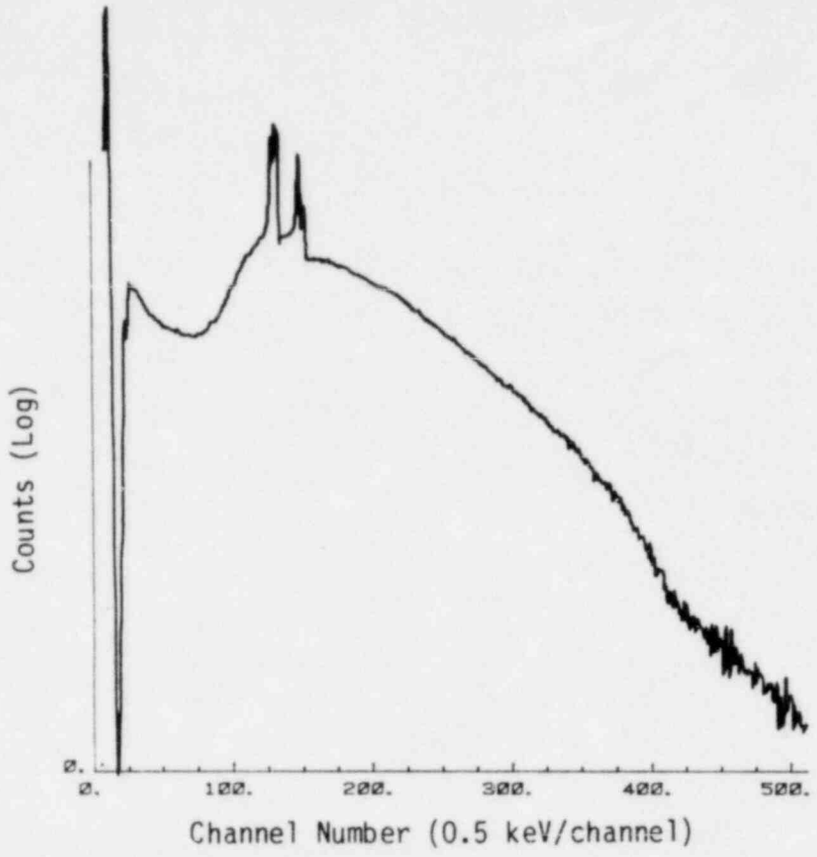

FIGURE A.7. Spectrum from NBS Technique MFK

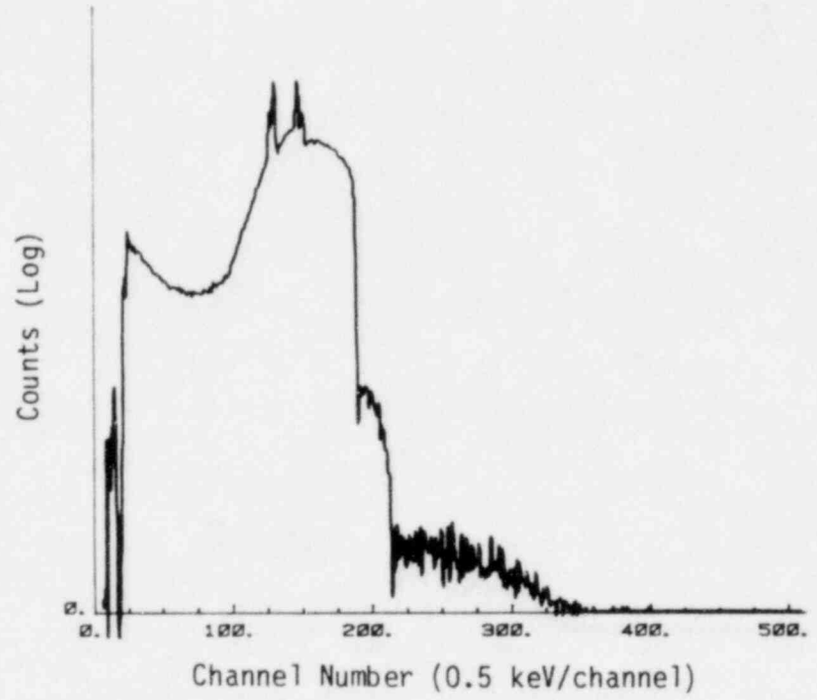

FIGURE A.8. Spectrum from NBS Technique HFE

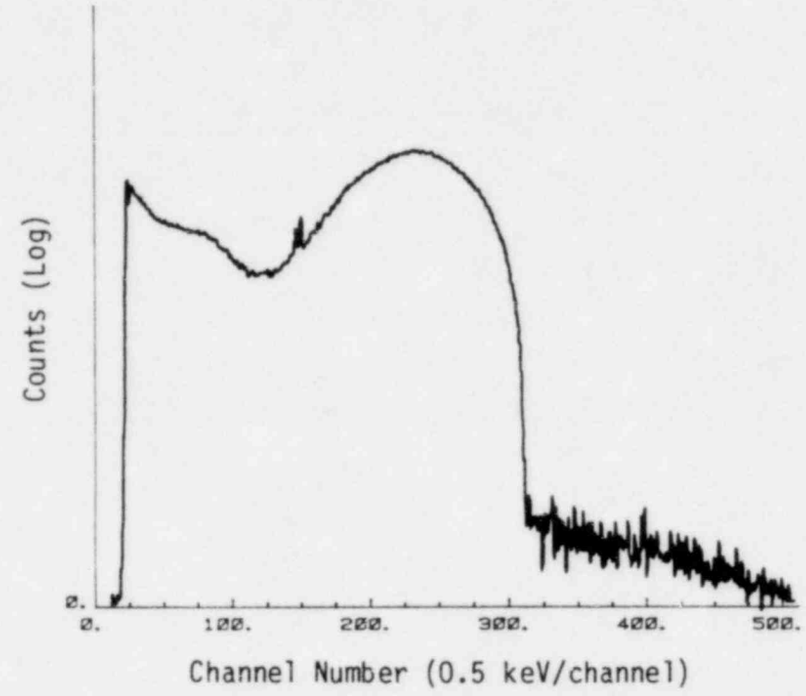

FIGURE A.9. Spectrum from NBS Technique HFG

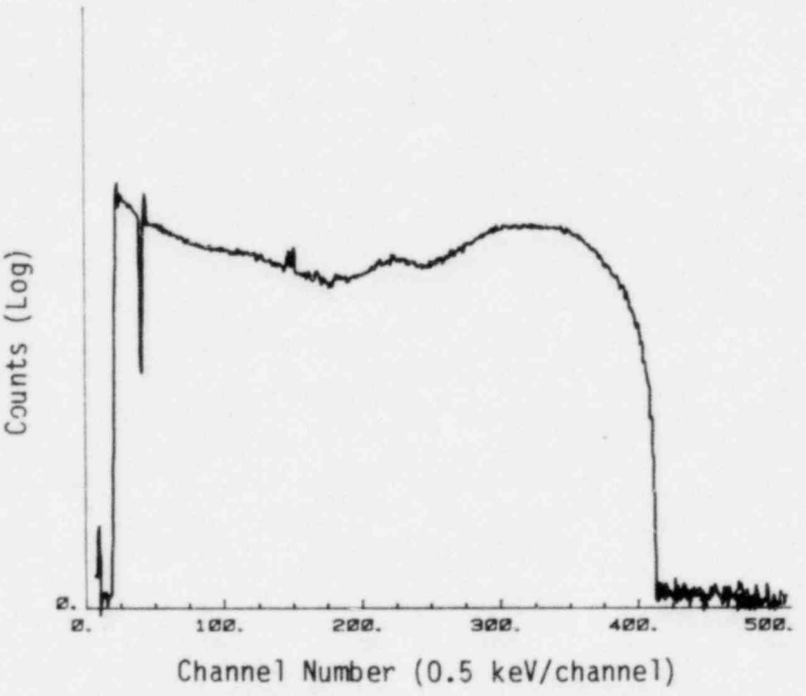

FIGURE A.10. Spectrum from NBS Technique HFI

TABLE A.2. PNL K X-Ray Techniques

Target Irradiator	kVp	K X-Ray Beam Filtration, mm	HVL, mm, Al	Assigned Energy, keV
Zr	60	None	0.059	16.1
Cd	95	None	1.219	23.7
La	115	None	3.04	34.3
Sm-Gd	125	0.8 Al	5.197	43
Ta	145	0.8 Al	8.672	58
Pb	165	2.4 Al 0.08 Cu	12.56	78
U	185	2.4 Al 0.08 Cu	14.19	100

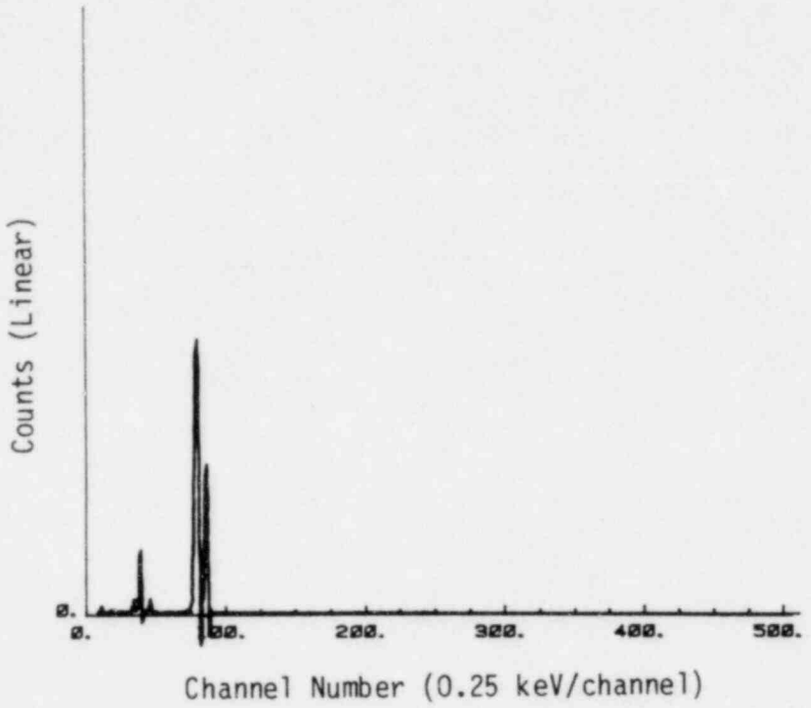

FIGURE A.11. Spectrum from 16.1-keV K X-Ray

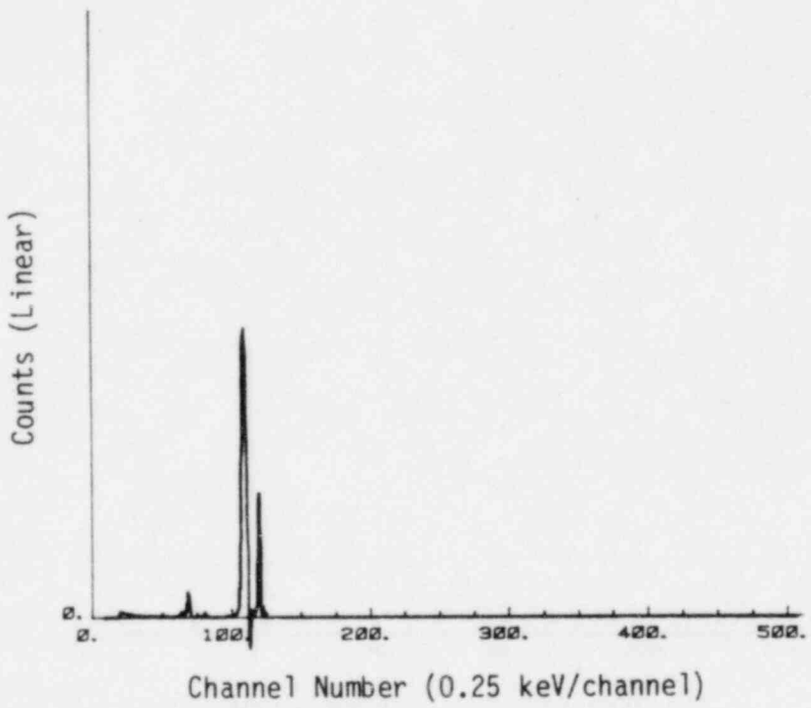

FIGURE A.12. Spectrum from 23.7-keV K X-Ray

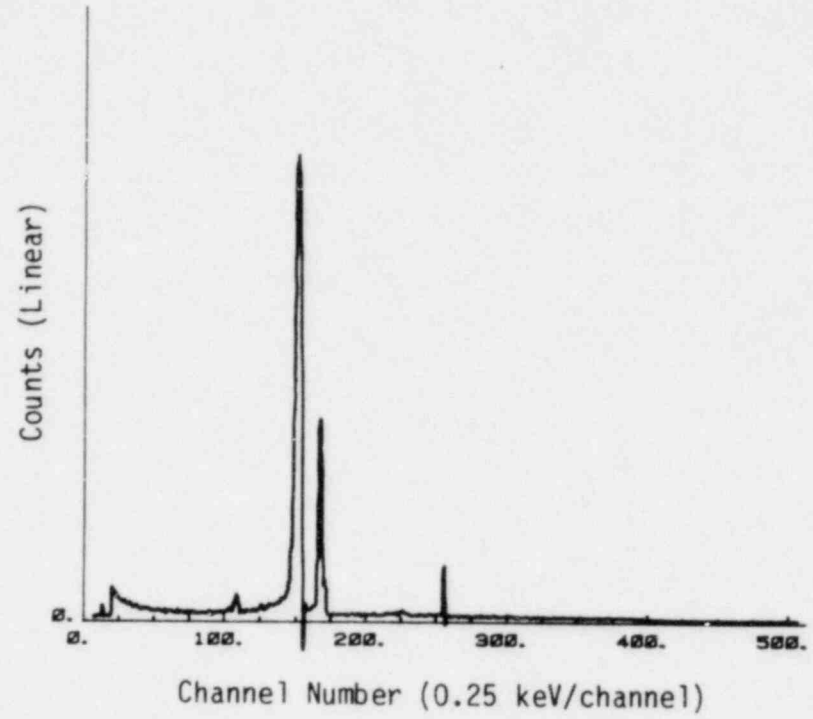

FIGURE A.13. Spectrum from 34.3-keV K X-Ray

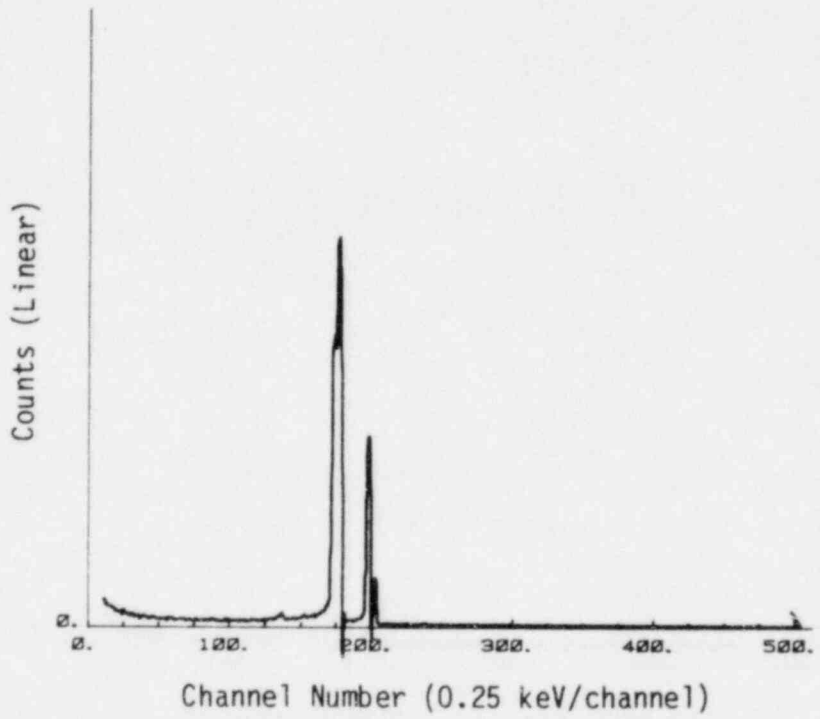

FIGURE A.14. Spectrum from 43-keV K X-Ray

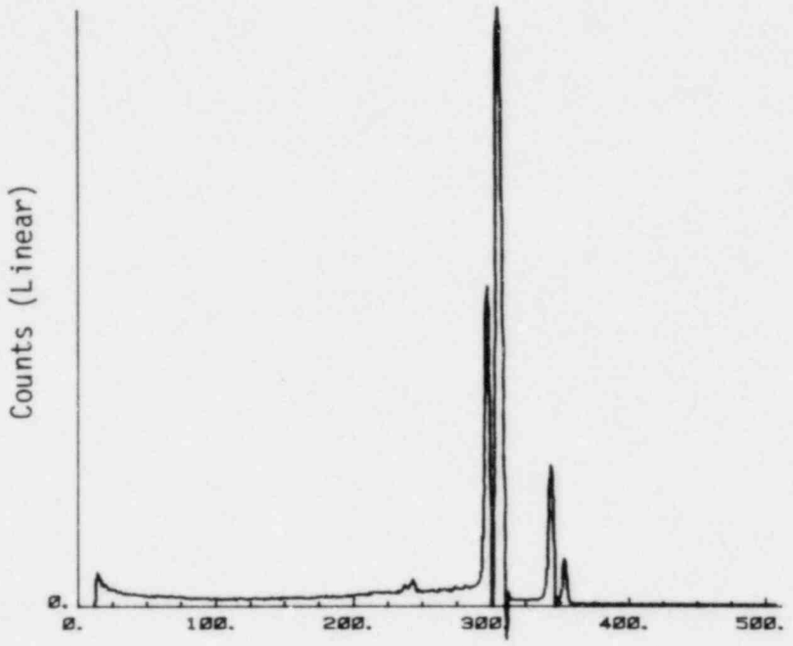

FIGURE A.15. Spectrum from 78-keV K X-Ray

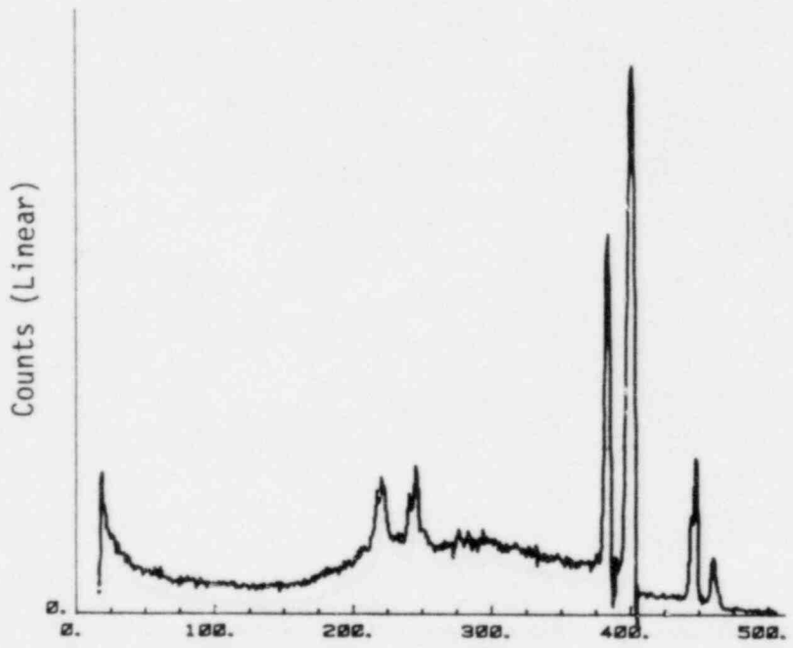

FIGURE A.16. Spectrum from 100-keV K X-Ray

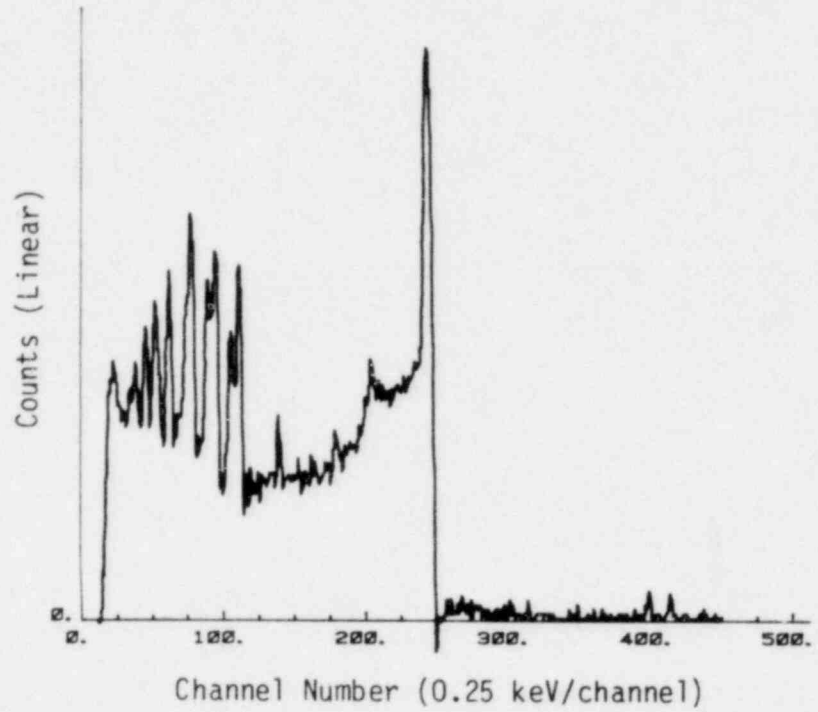

FIGURE A.17. Spectrum from Americium-241

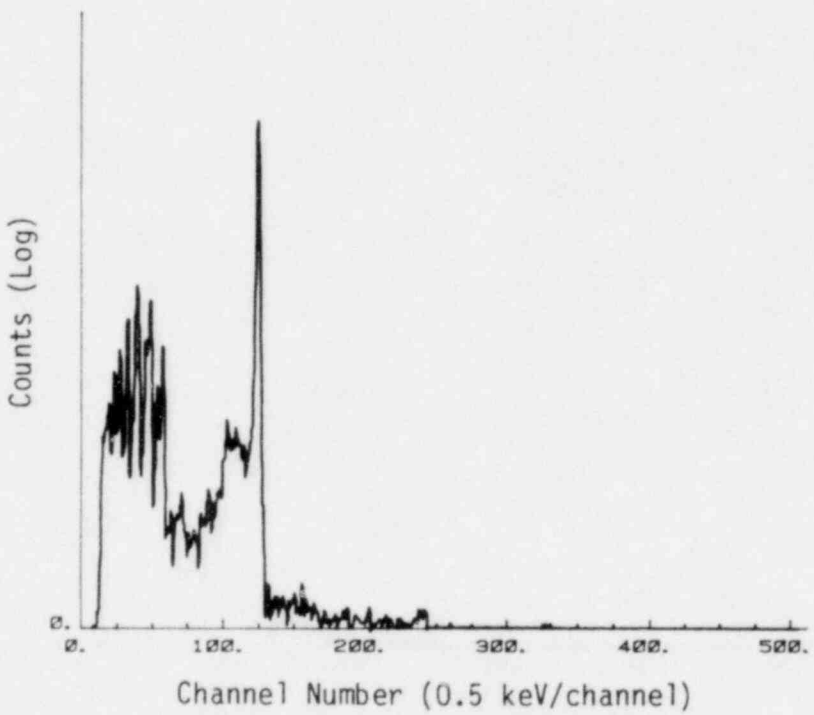

FIGURE A.18. Spectrum from Americium-241

APPENDIX B

TRANSMISSION OF K X-RAYS THROUGH TISSUE-EQUIVALENT PLASTIC

APPENDIX B

TRANSMISSION OF K X-RAYS THROUGH TISSUE-EQUIVALENT PLASTIC

The transmission of K x-rays through the tissue-equivalent plastic was measured to experimentally verify the suitability of the plastic as a tissue substitute. The measured transmission was compared to the expected transmission through muscle tissues. The muscle transmission was calculated from attenuation coefficients for muscle tabulated by Hubbell (1969). The tabulated coefficients used for specific energies of monoenergetic photons that did not correspond exactly to the K x-ray energies we used. Nonlinear interpolations of the tabulated attenuation coefficients for muscle were made to determine the coefficients applicable for our K x-ray energies. The attenuation coefficients derived from the tabulated data are presented below.

K X-Ray Energy, keV	Attenuation Coefficient, cm^{-1}
23.7	0.56
34.3	0.317
43	0.250
58	0.214
78	0.181

The following figures compare the measured transmission of K x-rays through the tissue-equivalent plastic with the expected transmission through muscle.

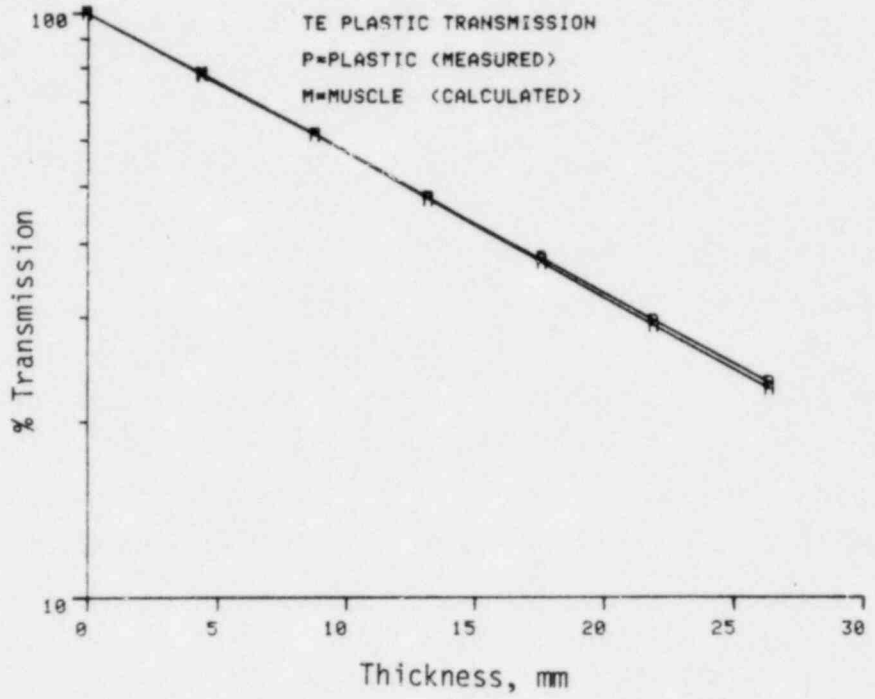

FIGURE B.1. Transmission Measurements for 23.7-keV K X-Rays

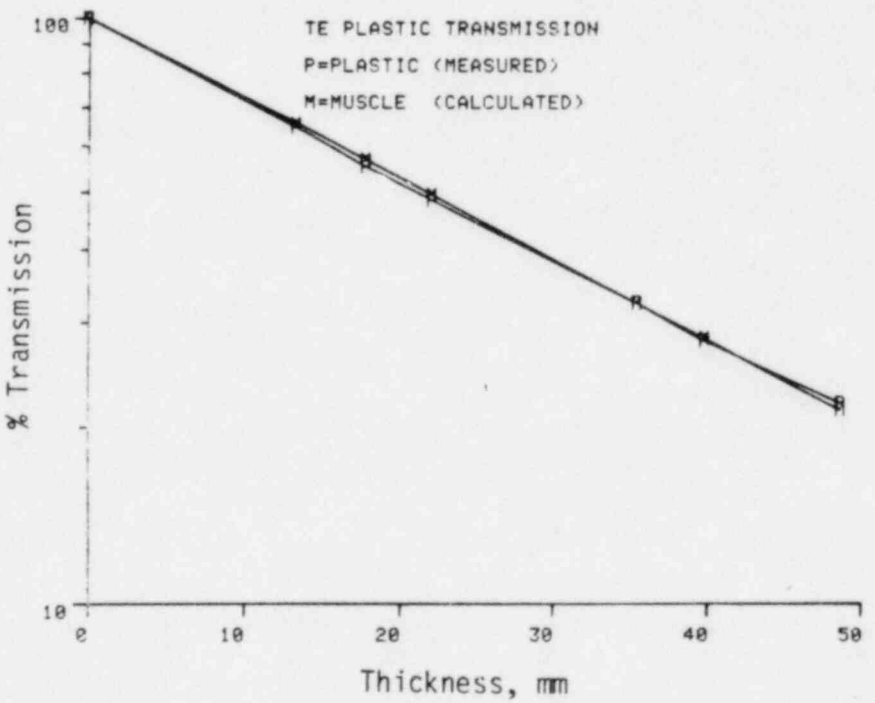

FIGURE B.2. Transmission Measurements for 34.3-keV K X-Rays

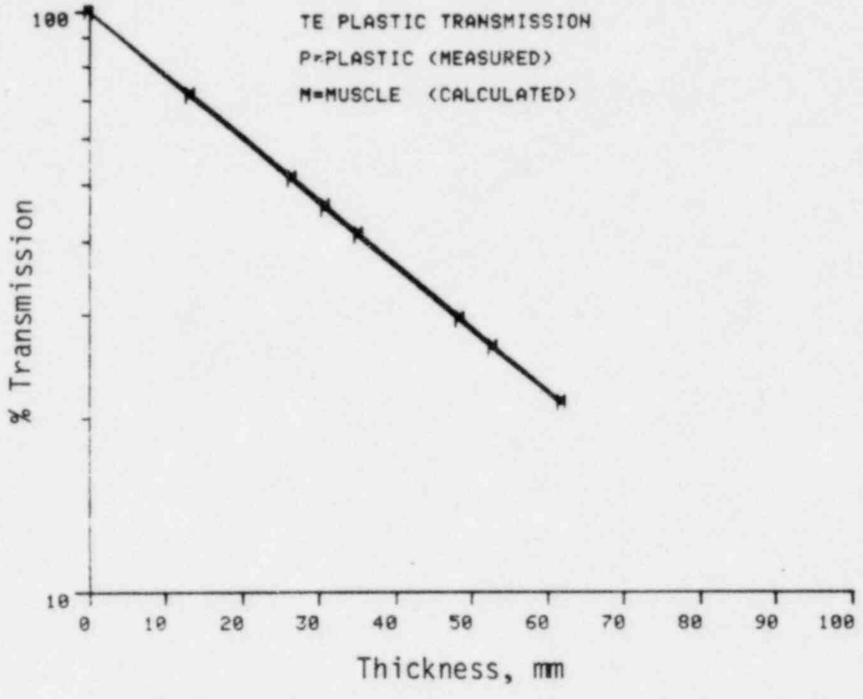

FIGURE B.3. Transmission Measurements for 43-keV K X-Rays

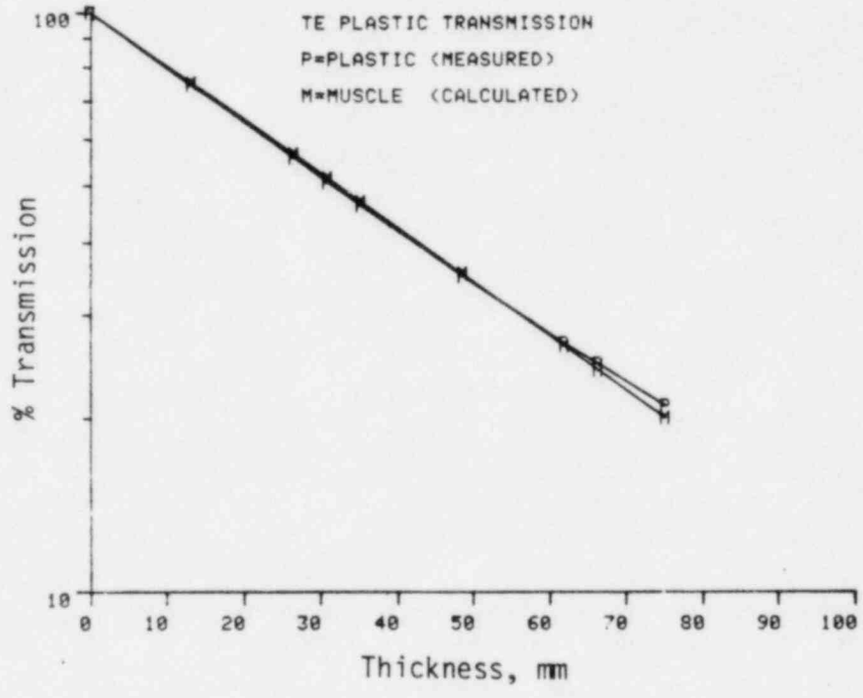

FIGURE B.4. Transmission Measurements for 58-keV K X-Rays

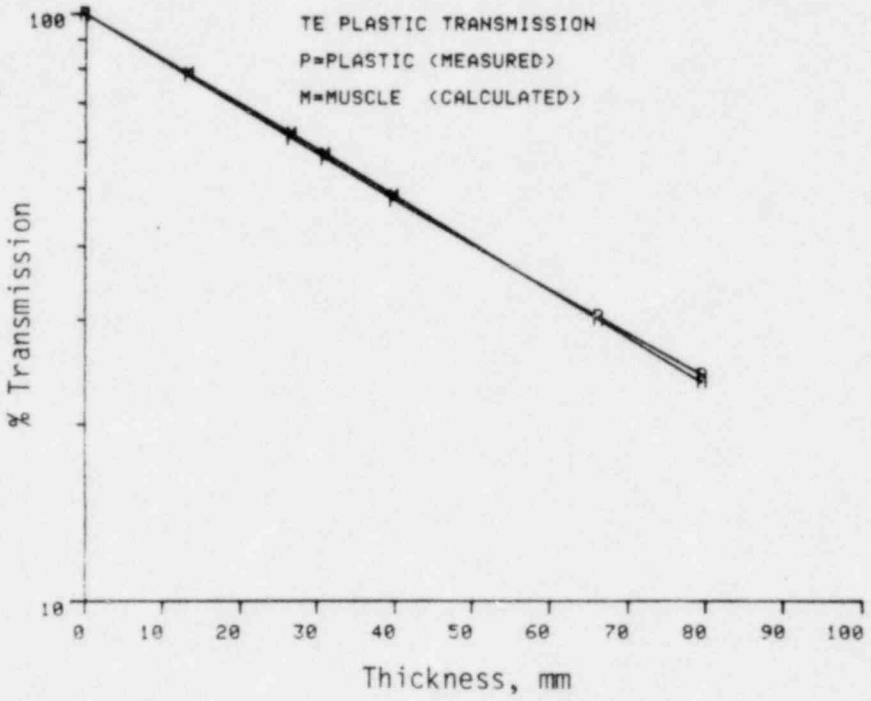

FIGURE B.5. Transmission Measurements for 78-keV K X-Rays

APPENDIX C

CALIBRATION DATA

APPENDIX C

CALIBRATION DATA

A. Filtered Techniques	R/C at 100 cm from Source
L-G	0.82×10^6
L-I	0.922×10^6
L-K	0.953×10^6
MFC	1.549×10^6
MFG	1.517×10^6
MFI	1.430×10^6
MFK	1.449×10^6
HFE	1.445×10^6
HFG	1.356×10^6
HFI	1.374×10^6

B. K X-Rays	R/C at 50 cm	R/C at 100 cm
16.1		1.122×10^5
23.7	5.542×10^5	1.185×10^5
34.3	5.353×10^5	1.351×10^5
43	5.641×10^5	1.503×10^5
58	5.464×10^5	1.488×10^5
78	4.699×10^5	1.293×10^5
100	3.966×10^5	1.115×10^5

APPENDIX D

CONVERSION FACTOR DATA

APPENDIX D

CONVERSION FACTOR DATA

The data in Tables D.1 and D.2 were derived from the extrapolation chamber measurements and were used in Equation 6 in the text to calculate the DEI conversion factors. The quantity E is the slope of the curve for ionization versus gap that was plotted for each x-ray energy and is tabulated in terms of 10^{-12} C/in. The quantity T is the charge collected in the transmission chamber for the corresponding E value and is tabulated in terms of 10^{-9} C. When used in Equation 6, both quantities were entered in terms of coulombs.

For the filtered x-rays, all measurements were made 100 cm from the x-ray source. For the K x-rays, the distance from the source was either 50 or 100 cm, depending on the intensity of the beam: for the energies 16.1, 23.7, and 34.3 keV, the tabulated data are for a distance of 100 cm; for the other K x-ray energies, the tabulate data are for a distance of 50 cm.

The average DEI conversion factors determined in this study are listed in Tables D.3 and D.4 for the K x-ray and filtered x-ray techniques, respectively. The DEI conversion factors in ANSI N13.11 are listed for comparison in Tables D.5.

TABLE D.1. Shallow DEI Data[a]

Filtered Technique	Trial 1		Trial 2		Trial 3	
	E	T	E	T	E	T
L-G	96760	500	124960	600	101280	500
L-I	113680	500	140800	600		
L-K	128240	500	129280	500		
MFC	5028	255	2412	125		
MFG	10338	500	10320	500	6388	300
MFI	13600	600	5480	250		
MFK	6524	300	6516	300		
HFE	4460	200	4376	200	4440	200
HFG	3192	150	2124	100		
HFI	2024	100	1489	75		
K X-Ray Energy						
16.1	1084	800	1732	1325		
23.7	969	686	1092	800		
34.3	400	250	1292	800	535	350
43	1406	174	1160	150		
58	1135	125	896	100		
78	840	100	820	100		
100	789	125	776	100	1040	150

(a) Values of E are in 10^{-12} C/in. Values of T are in 10^{-9} C.

TABLE D.2. Deep DEI Data[a]

Filtered Technique	Trial 1 E	Trial 1 T	Trial 2 E	Trial 2 T	Trial 3 E	Trial 3 T
L-G	40180	500	50640	600	41760	500
L-I	82800	500	100560	600		
L-K	105520	500	102880	500		
MFC	4728	255	2224	125		
MFG	10264	500	10560	500		
MFI	13740	600	5880	250		
MFK	6920	300	6684	300		
HFE	4720	200	4580	200		
HFG	3204	150	2132	100	2100	100
HFI	2036	100	1500	75		
K X-Ray Energy						
16.1	416	800	636	1325		
23.7	615	686	820	800		
34.3	378	250	1128	800	502	350
43	1432	174	1180	150		
58	1162	125	920	100		
78	900	100	868	100		
100	980	125	752	100	1134	150

(a) Values of E are in 10^{-12} C/in. Values of T are in 10^{-9} C.

TABLE D.3. Derived DEI Conversion Factors for K X-Ray Techniques

Energy, keV	Conversion Factor, rem/R	
	Deep (1.0 cm)	Shallow (0.007 cm)
16.1	0.38	1.08
23.7	0.74	1.07
34.3	0.99	1.07
43	1.30	1.28
58	1.54	1.47
78	1.72	1.61
100	1.74	1.59

TABLE D.4. Derived DEI Conversion Factors for NBS Filtered X-Ray Techniques

Technique	Energy, keV	Conversion Factor, rem/R	
		Deep (1.0 cm)	Shallow (0.007 cm)
L-G	15	0.45	1.08
L-I	21	0.81	1.13
L-K	26	1.0	1.21
MFC	32	1.07	1.15
MFG	42	1.25	1.25
MFI	64	1.47	1.41
HFE	70	1.46	1.38
MFK	84	1.44	1.35
HFG	117	1.41	1.41
HFI	167	1.31	1.31

TABLE D.5. DEI Conversion Factors Presented in ANSI N13.11

Energy, keV	Conversion Factor, rem/R	
	Deep (1.0 cm)	Shallow (0.007 cm)
15	0.16	0.79
20	0.45	0.87
30	0.94	1.07
40	1.18	1.25
50	1.28	1.32
80	1.38	1.38
100	1.37	1.37
200	1.27	1.27

APPENDIX E

TABULATED STOPPING-POWER DATA

APPENDIX E

TABULATED STOPPING-POWER DATA

A. Filtered X-Rays

Technique	Stopping-Power Ratio
L-G	1.175
L-I	1.177
L-K	1.176
MFC	1.179
MFG	1.176
MFI	1.168
MFK	1.162
HFE	1.166
HFG	1.156
HFI	1.151

B. K X-Rays

Energy, keV	Stopping-Power Ratio
16.1	1.174
23.7	1.176
34.3	1.178
43	1.175
58	1.170
78	1.163
100	1.159

DISTRIBUTION

No. of Copies

OFFSITE

A. A. Churm
DOE Patent Division
9800 S. Cass Avenue
Argonne, IL 60439

160 U.S. Nuclear Regulatory Commission
Division of Technical Information and Document Control
7920 Norfolk Avenue
Bethesda, MD 20014

2 DOE Technical Information Center

5 Robert Alexander
U.S. Nuclear Regulatory Commission
Office of Standards Development
5650 Nicholson Lane
Rockville, MD 20555

M. Ehrlich
U.S. Department of Commerce
National Bureau of Standards
Washington, D.C. 20234

E. J. Vallario
DOE Division of Occupation and Environmental Safety
Washington, D.C. 20545

No. of Copies

ONSITE

50 Pacific Northwest Laboratory

J. L. Baer
W. T. Bartlett (15)
J. M. Selby
C. M. Unruh
R. C. Yoder (25)
Technical Information (5)
Publishing Coordination (2)
Ei